FRONTIERS OF BIOGEOGRAPHY
The scientific journal of The International Biogeography Society

Frontiers of Biogeography 18, 2025, e141200 | DOI 10.21425/fob.18.141200

RESEARCH ARTICLE

Extending the Sea-Level Sensitive dynamic model of marine island biogeography to include fusion-fission islands

Sérgio P. Ávila[1,2,3,4], António Múrias dos Santos[5,6], Carlos S. Melo[1,4,7,8], João M. Porteiro[1,2,4], António M. Medeiros[1,2], Lara Baptista[1,2,3,9], Adriano Pimentel[10], Patrícia Madeira[1,2,3,4], A. Cristina Rebelo[1,3,4,11], Ana Hipólito[3,4], Sofie E. Voerman[12], Gonçalo C. Ávila[1,3,5], Mónica Moura[1,2,4], Björn Berning[1,3], Kenneth F. Rijsdijk[13], Esther Martín-González[14], Rui Quartau[8,15], Ricardo S. Ramalho[7,16], Markes E. Johnson[17]

1 *CIBIO, Centro de Investigação em Biodiversidade e Recursos Genéticos, InBIO Laboratório Associado, Pólo dos Açores, Azores, Portugal*
2 *Departamento de Biologia, Faculdade de Ciências e Tecnologia da Universidade dos Açores, 9501-801 Ponta Delgada, Açores, Portugal*
3 *MPB-Marine Palaeontology and Biogeography Lab, University of the Azores, Rua da Mãe de Deus, 9501-801 Ponta Delgada, Açores, Portugal*
4 *UNESCO Chair – Land Within Sea: Biodiversity and Sustainability in Atlantic Islands, Universidade dos Açores, R. Mãe de Deus 13A, 9500-321 Ponta Delgada, Portugal*
5 *Faculdade de Ciências da Universidade do Porto, 4169-007 Porto, Portugal*
6 *BIOPOLIS/CIBIO, Centro de Investigação em Biodiversidade e Recursos Genéticos, Rua do Crasto, 765, 4485-684 Vairão, Portugal*
7 *Departamento de Geologia, Faculdade de Ciências, Universidade de Lisboa, 1749-016 Lisboa, Portugal*
8 *Instituto Dom Luiz, Faculdade de Ciências, Universidade de Lisboa, 1746-016 Lisboa, Portugal*
9 *Royal Netherlands Institute for Sea Research, Landsdiep 4, 1797 SZ 't Horntje, Texel, Netherlands*
10 *Instituto de Investigação em Vulcanologia e Avaliação de Riscos (IVAR), Universidade dos Açores, Ponta Delgada, 9501-801, Portugal*
11 *SMNS - Staatliches Museum für Naturkunde Stuttgart, Rosenstein 1, 70191 Stuttgart, Germany*
12 *Lyell Centre for Earth and Marine Science and Technology, School of Energy, Geoscience, Infrastructure and Society (EGIS), Heriot Watt University, Research Avenue South, Edinburgh, EH14 4AP, UK*
13 *Department of Theoretical and Computational Ecology, Institute for Biodiversity and Ecosystem Dynamics, University of Amsterdam, 1090 GE Amsterdam, Netherlands*
14 *Museo de Ciencias Naturales de Tenerife, Organismo Autónomo de Museos y Centros, C/ Fuente Morales, 1, 38003 Santa Cruz de Tenerife, Canary Islands, Spain*
15 *Divisão de Geologia Marinha, Instituto Hidrográfico, Rua das Trinas, 49, 1249-093 Lisboa, Portugal*
16 *School of Earth and Environmental Sciences, Cardiff University, Cardiff, UK*
17 *Department of Geosciences, Williams College, Williamstown, MA 01267, USA*

Corresponding author: Sérgio P. Ávila (avila@uac.pt)

Editor Robert Whittaker
Received 18 November 2024 ♦ **Accepted** 23 June 2025 ♦ **Published** 12 September 2025

Abstract

This study extends the Sea-Level Sensitive dynamic model of marine island biogeography by integrating the dynamics of fusion-fission islands during glacial-interglacial cycles with marine island biogeography theory. We discuss the variations in littoral area due to Pleistocene sea-level changes and their effect on the evolutionary rates of splitting, extinction, and merging of populations, as well as on the speciation rates of marine shallow-water organisms. Here, we introduce three different types of fusion-fission islands: Solum islands, i.e., islands that have never been merged with neighbouring islands (at depths shallower than 50 m) during sea-level low stands associated with glacial episodes; Soror islands, i.e., islands that are subjected to fusion-fission cycles due to sea-level changes and thus may be functionally connected or separated depending on the amplitude of sea level changes; and Moliones islands, where two or more islands are functionally connected from a marine point of view, as the seafloor depth separating them is always shallower than 50 m, regardless of sea level. For this study, we selected 324 islands located in temperate and tropical climates, and representative of a broad geographic distribution, which were classified accordingly: 50 Solum islands, 77 islands making up 20 groups of Soror islands, and 197 islands from 34 groups of Moliones islands. Sea-level variation during glacial-interglacial cycles induced changes in the insular littoral area (ILA), resulting

in five general types of curves of ILA change herein described. These ILA curves depend on the depth distribution across the shelves, which, in turn, depends on several variables, including the age of the island, the tectonic setting, the presence of submarine and subaerial terraces, and also on the presence/absence of coral reefs. Finally, we provide several predictions on the frequencies of marine population splitting, extinction, and merging events, as well as on the speciation rates of shallow-water marine organisms, according to the respective island types.

Highlights

- We extend the Sea-Level Sensitive dynamic model of marine island biogeography theory to include the special case of fusion-fission islands.
- The dynamics of fusion-fission islands during glacial-interglacial cycles are relevant to evolutionary and biogeographic studies.
- We introduce new concepts (Solum, Soror, and Moliones islands) to designate islands according to the impact of glacial episodes and associated sea-level low stands on their marine biota.
- Five general types of curves of insular littoral area (ILA) change generated by sea-level variations during glacial-interglacial cycles are described.
- We hypothesize that the frequencies of marine population splitting, extinction, and merging events, as well as the speciation rates of shallow-water marine organisms, vary according to the island type.

Keywords

drivers of diversification, glacial-interglacial cycles, Island fusion-fission cycles, marine island biogeography, Moliones islands, sea-level oscillations, Solum islands, Soror islands

Introduction

From an evolutionary perspective, three main processes control the frequency of complete speciation events: 1) the rate of population splitting (i.e., initiation of within-species lineages); 2) the rate of population extinction; and 3) the rate of population merging (Dynesius and Jansson 2000) (Fig. 1). Based on the seminal works of MacArthur and Wilson (1963, 1967), it is well known by island biogeographers that, in the terrestrial realm, these rates vary according to a range of physical and geological characteristics of the island under study. Such factors include age, area, isolation, maximum elevation, topographical complexity, along with biological traits of the insular biota (including species richness, specialization level, and competition ability). Recent studies on the response of terrestrial environments to Quaternary glacial-interglacial cycles take into account the processes of island fusion-fission. This refers to the merging/fusion of two or more islands into a single island during glacial times, leading to an incremental increase in terrestrial area, and the consequences of division/fission into several islands during the subsequent interglacial period. These variations in island area resulting from sea-level changes produce significant impacts on the terrestrial biota (Rijsdijk et al. 2014; Papadopoulou and Knowles 2015, 2017; Fernández-Palacios et al. 2016; Simaiakis et al. 2017; Norder et al. 2019; Hammoud et al. 2021). However, analogous studies still await consideration for the marine realm. In addition, besides the ontogenetic classification of volcanic oceanic islands (into young, immature, mature, and old islands) proposed by Ávila et al. (2019), no attempt has been made so far to classify islands based on the configuration of the shelf. Such a classification would potentially impact our current understanding of the marine evolutionary and biogeographical dynamics in shallow-water organisms.

Marine island biogeography has recently witnessed a surge in topical interest (Ávila 2013; Hachich et al. 2015, 2016, 2020; Ávila et al. 2016, 2018; Florencio et al. 2021), resulting in novel models that aim to quantify biodiversity and to explain insular species distribution patterns as well as abiotic/biotic relationships (Patiño et al. 2017). Such novelties include the Vitória-Trindade Chain model (Pinheiro et al. 2017) and the Sea-Level Sensitive (SLS) dynamic model (Ávila et al. 2019). Several factors are known to influence shallow-water marine biodiversity on islands, including latitude, island age, isolation, presence/absence of coral reefs, and habitat heterogeneity. However, the most significant are insular littoral area (ILA) and eustatic sea-level changes, acting in tandem (Ludt and Rocha 2015; Ávila et al. 2018).

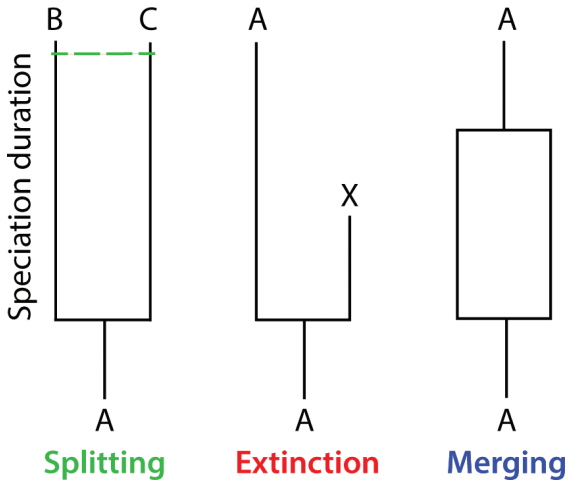

Figure 1. Representation of the three main processes that control the frequency of a complete event of speciation (sensu Dynesius and Jansson 2014): the frequency of population splitting, i.e., initiation of within-species lineages (shown in green), the frequency of population extinction (shown in red), and the frequency of population merging (shown in blue) (based on Papadopoulou and Knowles 2017).

As in previous studies (Ávila et al. 2018, 2019), ILA is herein defined as the submarine area located between the mean sea level (MSL) at any given time and its contemporaneous 50-m isobath. Ávila et al. (2018) explicitly recognised that ILA depends on the marine organism under study. At a depth of 50 m, a gradual shift in the composition of invertebrate species is observed, associated with a significant decrease in algal diversity, with only a few algal species dominating below this depth (Tittley et al. 2014). Thus, for biogeographic purposes, the lower limit for the calculation of ILA is 50 m for gastropods and algae, whereas for littoral species with wider bathymetric ranges (e.g., echinoderms and bivalves) it is 100 m. For littoral species with juveniles living in shallow water but adults living in deeper water (e.g., reef fishes), the lower limit of ILA should be placed at 200 m (Ávila et al. 2018, 2019). Among these marine organisms, molluscs have by far the best fossil record in insular habitats (Madeira et al. 2007), and have been the target of many recent biogeographic and evolutionary studies (e.g., Ávila 2006; Baptista et al. 2019, 2021; Melo et al. 2022, 2023; Sacchetti et al. 2023). Moreover, the effects of relative sea-level variations on ILA (one of the foci of this study) will be stronger when restricted lower limits are employed (Ávila et al. 2019). For these reasons, in this study, we continue to use the 50-m isobath for the calculation of the ILA.

The complex relationships between the most important abiotic variables and their impacts on the marine insular biota during evolutionary and ecological intervals are summarised in Fig. 2, as predicted by the SLS dynamic model of marine island biogeography (Ávila et al. 2019). The model integrates historical and ecological marine biogeography and is uniquely designed to account for the influence of glacial-interglacial cycles on shallow-water marine species richness. Central to the SLS model is the dynamic variation of the littoral area of oceanic islands (including hotspot islands, volcanic arc islands, and coral islands) and continental shelf islands (if far enough from the adjacent continental coastlines and if their pedestal is deep enough to preclude

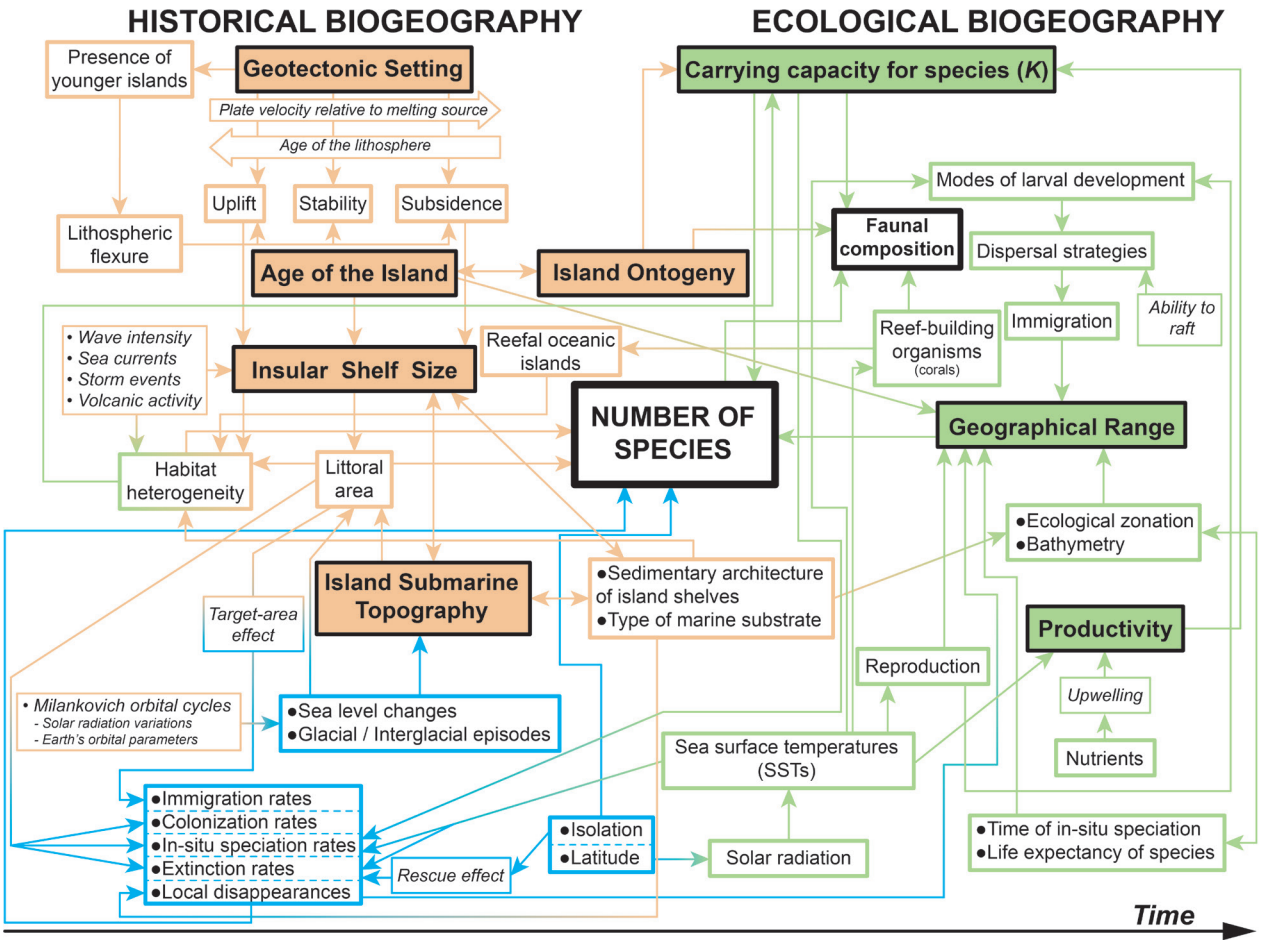

Figure 2. Flow diagram illustrating the intricate relationships among geological and biological variables as explored by the Sea-Level Sensitive (SLS) dynamic model of marine island biogeography (Ávila et al. 2019). The SLS was originally designed to study the special case of the reefless, volcanic oceanic islands. Although some of the variables expressed in this figure (e.g., the island ontogeny, the plate velocity relative to the melting source, the age of the lithosphere and the geotectonic setting) are only applicable to oceanic islands, all other variables and their inter-relations expressed in this figure equally apply to continental shelf islands. Thus, multiple geological and biological factors interact to shape insular biodiversity across evolutionary and ecological timescales. Key factors such as insular littoral area, latitude, age, and ontogenetic state (this only in the case of oceanic islands) play critical roles in determining species richness in shallow-water marine environments.

a land bridge effect) in response to sea-level oscillations driven by glacial-interglacial cycles, incorporating the physical effects of island ontogeny, as well as the associated submarine topography and marine substrate, on littoral biota. For a comprehensive review on these subjects, refer to Ávila et al. (2019) and Hachich et al. (2020).

Here, we discuss the effects of ILA changes as induced by glacial-interglacial cycles and the corresponding sea-level fluctuations affecting the biota of shallow-water insular habitats. In this study, we introduce three new concepts of distinct types of islands that yield a unique ILA dynamic signature over time (cf. Figs 3–5). "Solum islands" from the Latin, meaning "alone" (Fig. 3), are islands that have never merged with neighbouring islands during sea-level low stands associated with glacial periods and thus remained isolated during their entire geological history. Secondly, "Soror islands" from the Latin, meaning "sister" (Fig. 4), are islands that experience fusion-fission cycles due to sea-level changes, being isolated islands (fission) during interglacial periods, and becoming a single island (fusion) during glacial periods. In this case, the water depths between the islands are greater than 50 m. Thirdly, "Moliones islands", derived from Greek mythology, referring to the Siamese twins of Molione and Poseidon (Fig. 5), are two or more islands that remain functionally connected from a marine point of view, regardless of sea level changes. This connection is due to the shallow seafloor depths (less than 50 m) between them, effectively making them operate as a single island.

Methods

Selection of the islands

To assess the proposed concepts of Solum, Soror, and Moliones islands and their effect on marine evolutionary and biogeographical dynamics of shallow-water organisms, we selected a total of 324 islands for study (see Fig. 6). A key condition we imposed is that the selected islands were not severely impacted by ice during glacial times. Consequently, they are located in temperate and tropical climates that range in latitude from 47.74 °N (Ostrov Rasshua Island, Kuril Archipelago, Okhotsk Sea) to 20.19 °S (Aneityum Island, Vanuatu Archipelago). Further details can be found in Suppl. material 1: tables S1–S3. Within archipelagos, the selection of islands was random, as we did not use all the islands from the archipelagos sampled in this study. However, islands were not randomly picked from a table containing all islands on our planet, as this would not be feasible, considering the estimated 20,000 islands existing today with an area of over 1 km^2. Moreover, island selection fulfilled three important criteria. Firstly, they should be representative of a broad geographic distribution, with islands/archipelagos located in the Pacific and Atlantic Oceans, the Mediterranean Sea, the Japan Sea, the Okhotsk Sea, the Banda Sea and the Solomon Sea. Secondly, the dataset should include different types of islands, comprising ocean island volcanoes, island arc volcanoes, uplifted coral platforms, and continental shelf islands. Lastly, and for statistical reasons, after analysing the bathymetric data (see details below), we did our best to have at least 30 islands/groups of islands from each of the proposed categories (i.e., Solum, Soror and Moliones islands; see Suppl. material 1: tables S1–S3). This condition was fulfilled for Solum (50 islands) and Moliones (32 groups of islands) but not for Soror (20 groups of islands), despite our best efforts to do so.

Calculation of the insular littoral area

The insular littoral area (ILA) of Solum islands or groups of islands (in the case of Soror and Moliones) was calculated for the last 150 ka (thousands of years). Following Ávila et al. (2018)m we define ILA as the area corresponding to the insular shelf surface located between the mean sea level (MSL) at a given time and the contemporary 50-m isobath. Thus, this 50-m spread in bathymetric range encompasses the intertidal down to the infralittoral biological zones. Calculations were performed using QGIS 3.28.8 (QGIS 2023). For bathymetric data, we used the GEBCO 2023 Grid, which is a global terrain model for ocean and land, providing elevation data, in meters, on a 15 arc-second interval grid (GEBCO 2023). When compared to shallow-water shipborne multi-beam bathymetry, GEBCO 2023 represents a lower resolution database, with a spatial resolution of about 1 km at the equator. Nevertheless, it is the only bathymetric/topographic dataset with global coverage and sufficient resolution to support a comprehensive comparative study such as presented here.

For each island/group of islands, we manually checked the location of the bathymetric lines of -50 m, -120 m, and -170 m, defined the limits of the polygon encircling these depths, and classified all selected islands/groups of islands as Solum, Soror, or Moliones. The -120 m bathymetric line is related to the deepest level attained during the Last Glacial Maximum (Miller et al. 2011), while the -170 m line is related to the littoral area during this period (i.e., the first submerged 50 m). In total, 31 bookmarks were employed (cf. Fig. 6), including all the islands/groups of islands that were previously selected. For each bookmark, shapefiles were used to extract bathymetric data from the global GEBCO database. A GDAL algorithm ("gdal_contour"; GDAL/OGR version 3.8.3) was employed to generate the polygon used to calculate the littoral area between the two sea levels (reference level and -50 m). In total, the GDAL algorithm was run 4,681 times (31 bookmarks × 151 ka), making it possible to determine the size (in km^2) of littoral surface areas (0–50 m depth) over the last 150 ka through time steps of 1 ka, based on the sea-level curve developed by Miller et al. (2011).

For simplicity, our approach considers that no morphological changes occurred in the islands, i.e., that the present-day topography/bathymetry of an island remained the same throughout the examined time interval. Accordingly, our analyses did not account for any potential changes in topography or bathymetry resulting from erosion,

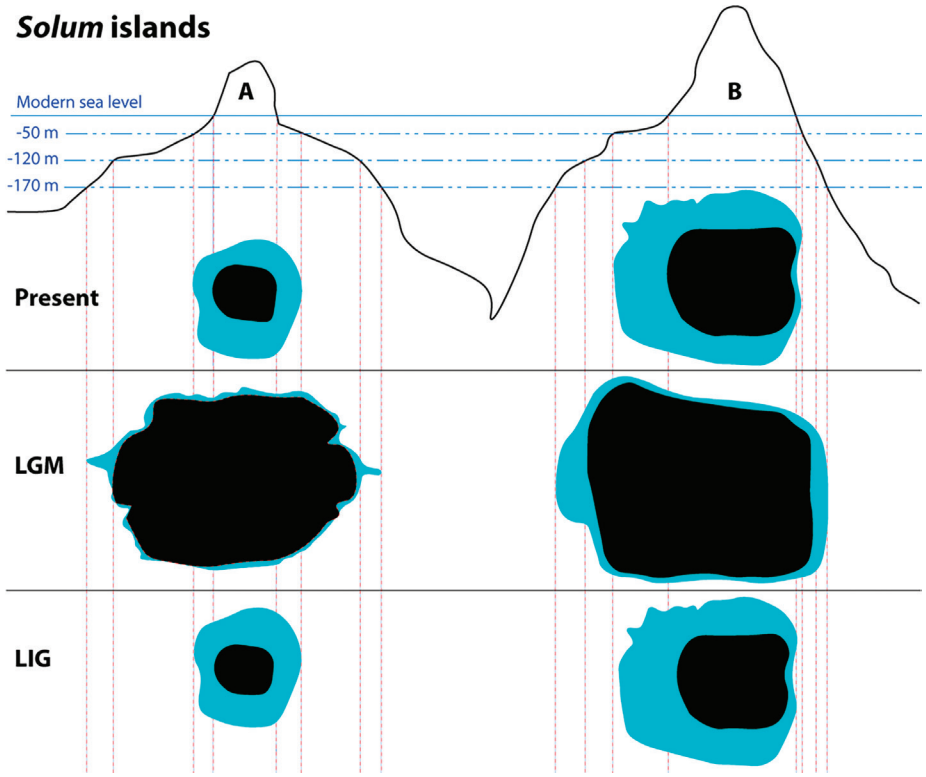

Figure 3. Hypothetical representation of the insular littoral area (in blue) and subaerial area (in black) variation for Solum islands during three different periods: the modern times (Present), the Last Glacial Maximum (LGM), and the Last Interglacial (LIG).

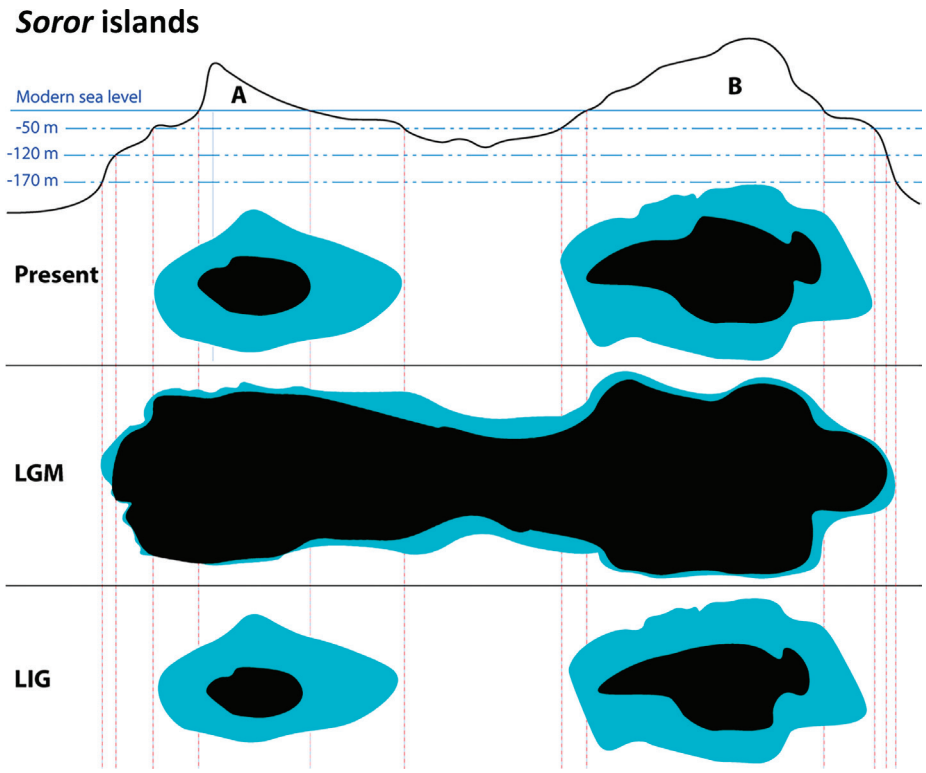

Figure 4. Hypothetical representation of the insular littoral area (in blue) and subaerial area (in black) variation for Soror islands during three different periods: the modern times (Present), the Last Glacial Maximum (LGM), and the Last Interglacial (LIG).

sedimentation, landslides, volcanic and tectonic activity, coral reef growth, or other processes that may have occurred during the time interval under consideration. Similarly, we did not take into account any uplift or subsidence movements in our analyses, even though it is well recognised that such isostatic movements may play a role in modifying the littoral area of an island over a significant period of time (Ramalho et al. 2013; Quartau et al. 2016, 2018; Ávila et al. 2019).

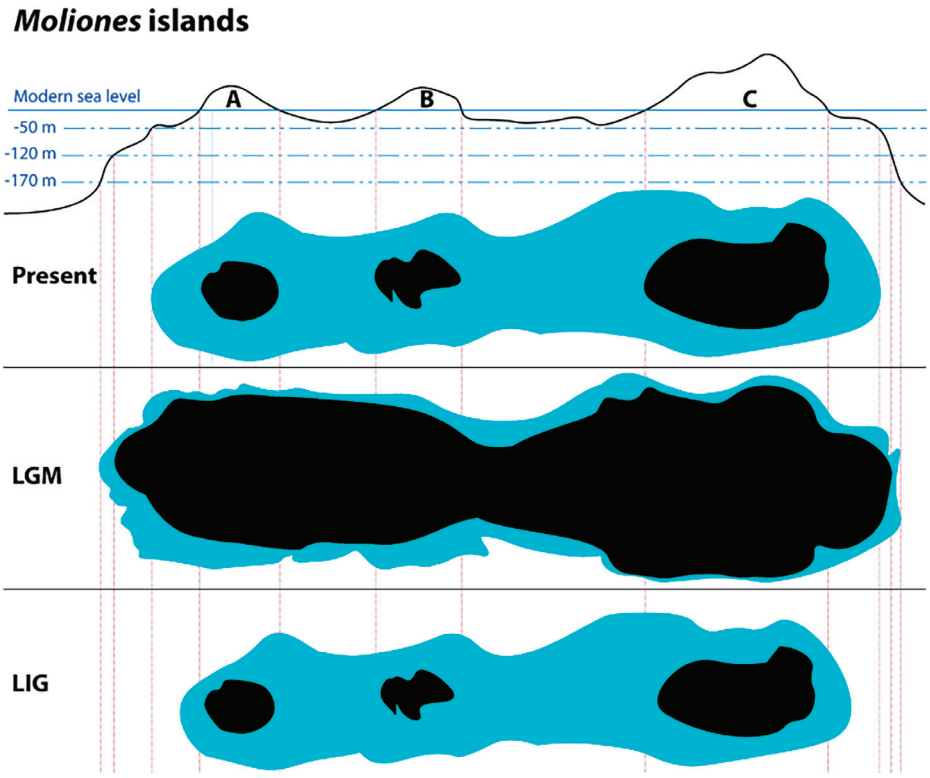

Figure 5. Hypothetical representation of the insular littoral area (in blue) and subaerial area (in black) variation for Moliones islands during three different periods: the modern times (Present), the Last Glacial Maximum (LGM), and the Last Interglacial (LIG).

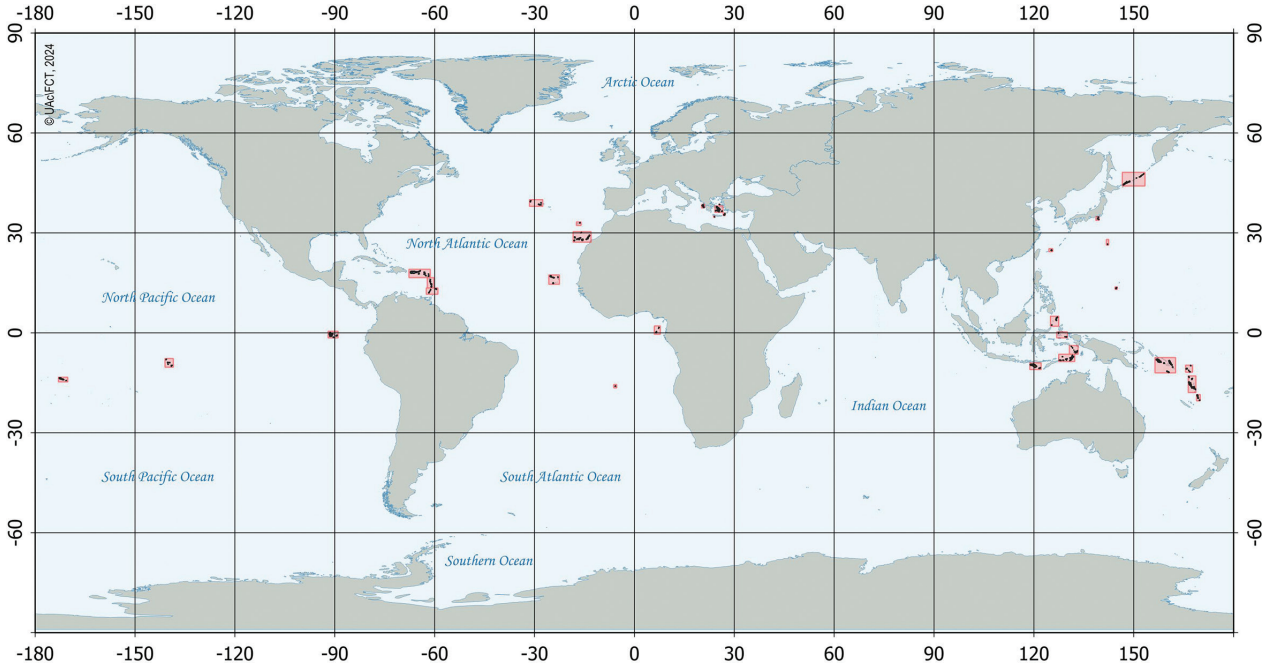

Figure 6. World map showing the geographic location of all 324 islands (in black and inside red boxes) used in this study. For a detailed map of each island, please see Suppl. material 1: figs S8–S38.

Statistical approach to the classification of the insular littoral area curves

We followed an iterative process to classify all ILA variation curves, as depicted in Suppl. material 1: figs S1–S6. First, all ILA curves were log-transformed (Suppl. material 1: fig. S7). We calculated the polynomial curves for each of the 104 ILA variation curves used in this study (50 Solum ILA curves, 20 Soror ILA curves, and 34 Moliones ILA curves). The curve used was a 5th degree polynomial of the type: $ILA = ax^5 + bx^4 + cx^3 + dx^2 + ex + f$. We also fitted this 5th degree polynomial curve against

each ILA curve and calculated the value of r^2. A table was then constructed for each of the 104 ILA curves, with the values of the terms (a, b, c, d, e, f) for each polynomial curve, plus the calculated r^2 (Suppl. material 1: table S4). Then, Principal Components Analysis (PCA) was performed on Suppl. material 1: table S4 values (Fig. 7). Finally, we double-checked the results of the PCA against each ILA curve by visual inspection and corrected any misclassifications.

Comparison of ILA curves: GEBCO versus high-resolution bathymetry

We tested if the use of the GEBCO 2023 grid, which has a poor bathymetric resolution of about 1 km at the equator, could compromise the fidelity of our data, as for some islands with narrow insular shelves, the calculated ILA curves could be rough speculations. To assess this, we compared the ILA curves for Santa Maria Island in the Azores Archipelago, an example of a Solum island where high-resolution bathymetry is available (8 m resolution; Ricchi et al. 2020), with those generated from GEBCO 2023. A similar comparison was done for the ILA curves of the Pico+Faial Soror islands (Azores Archipelago), for which we have a compilation of high resolution multibeam bathymetry (50 m resolution; cf. Quartau et al. 2015), with those obtained from GEBCO 2023.

Results

Solum, Soror, and Moliones islands

Of the 324 islands surveyed, 50 fall into the category of Solum islands (as listed in Suppl. material 1: table S1), 77 islands form 20 groups of Soror islands (Suppl. material 1: table S2), and the remaining 197 are grouped into 34 Moliones islands (Suppl. material 1: table S3). The number of islands classified as Soror within an insular system varies, ranging from two (e.g., Pico and Faial, collectively known as "Laurinsula" (Ávila et al. 2018), in the Azores Archipelago) to a maximum of 19 islands located in the Aegean Sea (Andros, Mykonos, Tinos, Syros, Rineia, Strongyli, Despotiko, Antiparos, Paros, Naxos, Donousa, Keros, Schoinoussa, Irakleia, Ios, Kato Koufonisi, Ano Koufonisi, Sikinos, and Folegandros); see also Suppl. material 1: table S2. The number of islands within Moliones systems range from two in the Caribbean Sea (e.g., Puerto Rico and Virgin Islands) to a maximum of 34 islands also in the Caribbean Sea (Grenada, Caille Island, Ronde Island, Les Tantes, Diamond Island, Large Island, Frigate Island, Saline Island, White Island, Carricou, Mabouya, Sandy Island, Petit Dominique, Fota, Petit Martinique, Petit Saint Vincent, Palm Island, Union Island, Petit Tabac, Jamesby, Petit Tameau, Baradal, Mayreau, Catholic Island, Canouan, Savan Island, Petit Mustique, Mustique, The Pillories, All Awash Island, Baliceaux, Battowia, Isle A Quatre, and Porth Elizabeth); cf. Suppl. material 1: table S3.

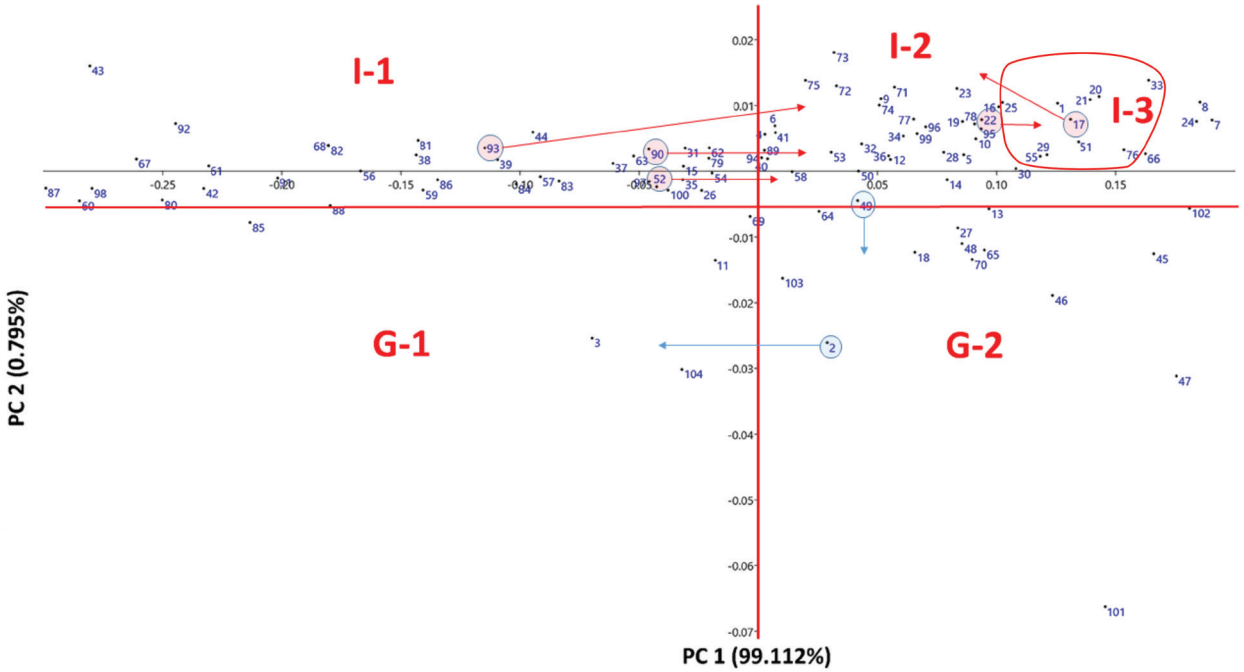

Figure 7. Results of the Principal Components Analysis (PCA) performed on Suppl. material 1: table S4 values. Numbers refer to Solum, Soror, and Moliones islands (please check Suppl. material 1: table S4). PCA is able to discriminate between I-1, I-2, G-1 and G-2, whereas I-3 was only detected by eye inspection and is a subgroup within the I-2 ILA curves. From all studied islands/groups of islands classified as I-1, I-2, I-3, G-1 or G-2 (see "General types of insular littoral area curves" section in the main manuscript), the use of PCA coupled with visual inspection shows that only 7 of the 104 Solum, Soror, and Moliones islands (i.e., about 6.7%) are not well classified; in these cases, the PCA classification was corrected by visual inspection. The incorrectly classified islands/groups of islands by PCA are shown in red circles (in the case of I-type ILA curves) and in blue circles (in the case of G-type ILA curves).

General types of insular littoral area curves

Four main types of ILA curves were detected using Principal Component Analysis, depicting changes in the ILA in response to sea-level variations during glacial-interglacial cycles. Islands that conformed to the SLS prediction, as their littoral area attained maximum values during interglacial periods, were classified as I-type (Table 1). In contrast, if the littoral area reached its maximum values during glacial periods, the islands were classified as G-type. "I" stands for Interglacial and "G" stands for Glacial. The PCA detected four main ILA curves: two for I-type islands (Fig. 7I-1, I-2), and two for G-type islands (Fig. 7G-1, G-2).

When the PCA results were compared with each ILA curve by visual inspection, it was clear that one more general ILA curve (I-3) was discernible. Moreover, this comparison revealed that seven out of the 104 islands/groups of islands classified according to the PCA were not well categorised and some changes were required: three ILA curves classified by PCA as I-1 were changed to I-2; one ILA curve classified by PCA as I-2 was changed to I-3; one ILA curve classified by PCA as I-3 was changed to I-2; one ILA curve classified by PCA as I-2 was changed to G-2; and finally, one ILA curve classified by PCA as G-2 was changed to G-1 (cf. Table 1).

Thus, this study identified five general types of curves (Fig. 8), which are described below:

i. ILA curve type I-1 (Fig. 8I-1) is characterised by two maximum values of littoral area: the highest and also the oldest at around 122–126 kyr (during the warmest period of the Last Interglacial, i.e., the MIS 5e), and the most recent from 2–6 kyr up to the present time. There is a sharp increase in littoral area values during part of Termination II (from 132 to 126 kyr), and during a period lasting from 18 to 2–6 kyr (spanning Termination I (18–9 kyr) and part of the Holocene). Terminations correspond to short periods of time (usually 5–6 kyr) when there is a rapid transition from a full glacial climate to a full interglacial climate. Near the end of the Last Interglacial period, at around 122 ka, there is a sharp decrease in ILA values, resulting in a near-constant minimum from 116 to 18 kyr, a large period covering the end of the Last Interglacial (LIG) and the whole Last Glacial period (LG), which includes the marine isotopic stages (MIS) 4 (57–71 kyr), MIS 3 (29–57 kyr), and MIS 2 (11.7–29 kyr). Two small peaks in ILA might occur in some islands, the first at around 105–93 kyr (which includes the peak of interglacial sub-stage MIS 5c, at 96 ka) and the second at around 87–73 kyr (which includes the peak of interglacial sub-stage MIS 5a, at 82 ka);
ii. ILA curve type I-2 (Fig. 8I-2) mimics the sea-level curve. The main difference between curves type I-1 and I-2 resides in the much higher values of the peaks of ILA at around 105–93 kyr and at around 87–73 kyr of curves type I-2. On many islands or groups of islands, variations in ILA also occur during the LIG period, from 130 to 116 kyr. Additionally, at the end of the LG period, the littoral area peaks at around 11–9 kyr, thus earlier than curve type I-1;
iii. ILA curve type I-3 (Fig. 8I-3) was discovered by eye inspection and is characterised by a sharp decrease in littoral area values during the warmest period of the LIG (around 129–127 to 115–118 kyr), as well as at present time, in stark contrast to curve types I-1 and I-2. Maximum ILA values are reached in several, nearly equal, peaks, during a large timeframe, from 131 to 81–75 kyr. In a similar way to ILA curve type I-2, the littoral area also peaks in I-3 curves at around 11–9 kyr, and then its values decrease to the present time;
iv. ILA curve type G-1 (Fig. 8G-1) is characterised by minimum values of littoral area during the LIG period, with values analogous to those of the present interglacial. Moreover, littoral area peaks at several, similar, maximum values for a long period that extends from 113–112 to 15–14 kyr, thus including both glacial (MIS 2 to MIS 4) and minor interglacial periods (MIS 5a and MIS 5c);
v. ILA curve type G-2 (Fig. 8G-2) is almost symmetrical to the sea-level curve. Moreover, the main difference between the two types of G-curves is that in G-2, there is a steady increase in littoral area values from the minimum ones, observed at around 131–126 kyr, to the maximum values, reached between 20–15 kyr. In addition, all G-2 islands are characterized by variable, intermediate values of ILA associated with MIS 5d (112–107 kyr) and MIS 5b (91–86 kyr).

Table 1. Classification of Solum, Soror, and Moliones islands according to the type of curve deduced for the littoral area variation for the last 150 ka. Refer to the main text for detailed descriptions of each type of curve.

Type of islands	Maximum littoral area attained during:		Total number of islands	Curve type					Total number of islands
	I - interglacials	G - glacials		I-1	I-2	I-3	G-1	G-2	
Solum (Total)	39	11	50	10	21	7	3	8	49
***Solum* (%)**	***78.0***	***22.0***	***100.0***	***20.4***	***42.9***	***14.3***	***6.1***	***16.3***	***100.0***
Soror (Total)	16	4	20	10	4	2	1	3	20
Soror (%)	***80.0***	***20.0***	***100.0***	***50.0***	***20.0***	***10.0***	***5.0***	***15.0***	***100.0***
Moliones (Total)	27	5	32	13	13	1	1	4	32
***Moliones* (%)**	***84.4***	***15.6***	***100.0***	***40.6***	***40.6***	***3.1***	***3.1***	***12.5***	***100.0***

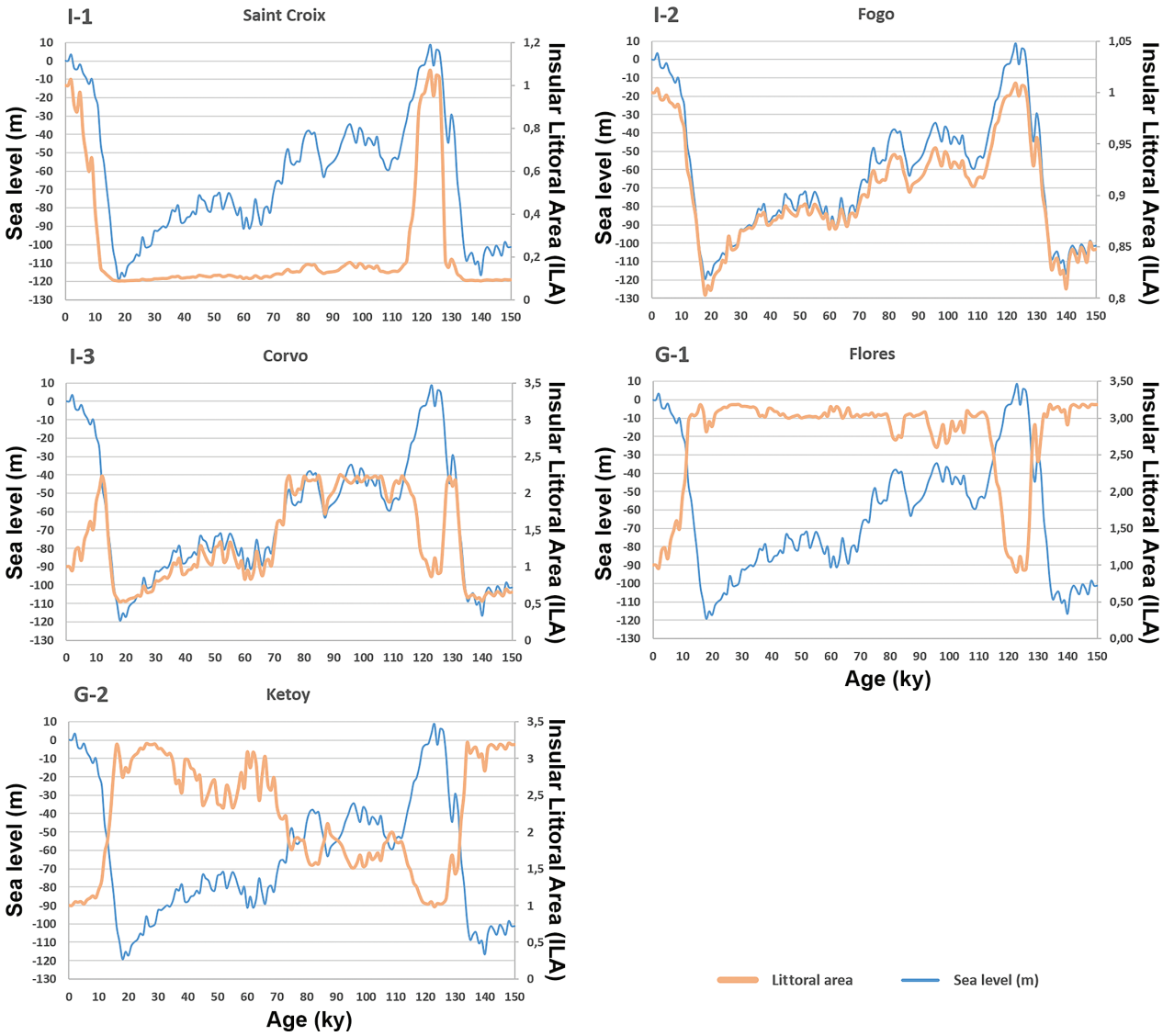

Figure 8. Main types of curves for Insular Littoral Area variation (ILA, in km^2) over the last 150 ka are depicted in orange. Sea level variation curve based on Miller et al. (2011), is shown in blue.

Classification of Solum, Soror, and Moliones islands, according to the types of curves of littoral area variation

In the following sections, we classify Solum islands, as well as Soror and Moliones groups of islands, according to the types of curves of littoral area variation for the last 150 ka based on the PCA and visual inspection of the ILA curves.

(*1*) *Solum Islands*. Suppl. material 1: figs S1–S3 display the results of the ILA variation curves in 50 Solum islands for the last 150 ka. Of these, 39 islands conformed to the SLS dynamic model predictions and were classified as I-type, whilst the remaining 11 islands were classified as G-type (Table 1). We classified 49 of the 50 Solum islands (cf. Table 1; see Suppl. material 1: table S1 for classification of each island) according to the following types of ILA curves. The ILA curve type I-1 is exemplified by 10 out of the 49 classified Solum islands (20.4% in total; Table 1): Saint Croix, Sal, Ua Huka, Tanna, Nendo, Utupua, Naunonga, Sumba, Damar, and Teun. The ILA curve type I-2 (Fig. 8I-2) is exemplified by 21 islands (42.9%; Table 1): Saba Island, Marie Galante, Dominica, Martinica, Saint Lucia, Barbados, Santo Antão, Fogo, La Palma, El Hierro, Tenerife, São Tomé, Santiago, Moho Tani, Ua Pou, Nuku Hiva, Aneityum, Erromango, Rennel Island, Malaita, and Guam. In most islands (e.g., Saba, Martinica, Barbados, La Palma, El Hierro, and São Tomé), variations in ILA also occurred during the Last Interglacial period. The ILA curve type I-3 (Fig. 8I-3) is represented by seven islands (14.3%; Table 1): Corvo, Gran Canaria, Selvagem Pequena, Selvagem Grande, Porto Santo, Príncipe, and American Samoa. The ILA curve type G-1 (Fig. 8G-1) is represented by three islands (6.1%; Table 1): Flores, Graciosa, and Saint Helena. Finally, ILA curve type G-2 (Fig. 8G-2) is represented by eight islands (16.3%; Table 1): São Nicolau, La Gomera, Isla Floreana, Etorofu (=Iturup), Ostrov Simushir, Ketoy, Izu Oshima, and Miyake.

(*2*) *Soror Islands*. Suppl. material 1: fig. S4 displays the results of the ILA variation curves of 20 groups of Soror islands for the last 150 ka. Of these, 16 groups of islands conformed to the SLS dynamic model predictions and were classified as I-type, as their ILA attained maximum values during interglacial periods. In contrast, the littoral area of four groups of islands (Gavdos+Gavdopoula islands, and the Cyclades, Lesser Sunda, and Izu archipelagos) reached its maximum values during glacial periods, and were classified as G-type (Table 1 and Suppl. material 1: table S2). We were able to classify all of the 20 groups of Soror islands (Table 1). ILA curve type I-1 is exemplified by 10 out of the 20 groups classified as Soror islands (50.0%), curve type I-2 is exemplified by four groups of Soror islands (20.0%), curve type I-3 is exemplified by two groups of Soror islands (10.0%), curve type G-1 is exemplified by one group of Soror islands (5.0%), and finally, curve type G-2 is exemplified by three groups of Soror islands (15.0%). See Suppl. material 1: table S2 for the discrimination of islands per group of Soror islands, as well as the classification of the ILA curve types.

(*3*) *Moliones Islands*. Suppl. material 1: figs S5, S6 display the results of ILA variation curves of 34 groups of Moliones islands for the last 150 ka (Suppl. material 1: table S3). We found that 27 groups conformed to the SLS dynamic model predictions, and were classified as I-type, whereas five groups of islands were classified as G-type (Table 1). We were able to classify 32 of the 34 groups of Moliones islands (cf. Table 1). Curve type I-1 is exemplified by 13 out of the 32 groups classified as Moliones islands (40.6%), curve type I-2 is exemplified by 13 groups of Moliones islands (40.6%), curve type I-3 is exemplified by one group of Moliones islands (3.1%), curve type G-1 is exemplified by one group of Moliones islands (3.1%) and finally, curve type G-2 is exemplified by four groups of Moliones islands (12.5%). See Suppl. material 1: table S3 for the discrimination of islands per group of Moliones islands as well as the classification of the littoral area curve types.

Comparison of ILA curves: GEBCO versus high-resolution bathymetry

Despite its relatively coarse resolution, the ILA curves derived from GEBCO 2023 (Fig. 9A, B) are broadly consistent with those obtained from much higher resolution data (Fig. 9C, D). Although some small differences are noticeable, crucially, the overall shape and behaviour of the ILA curves remain similar (cf. Fig. 9). While future advancements in global terrain models will likely enhance the accuracy of this methodology, GEBCO 2023 currently represents the most comprehensive and up-to-date global dataset available. Accordingly, it was the most appropriate choice for the bathymetric analysis of the islands in this study.

Discussion

Impact of sea-level variations on Solum, Soror, and Moliones islands

Sea-level changes driven by glacial-interglacial cycles increased in frequency and amplitude during the last one million years of the Pleistocene (Miller et al. 2011). This period marked a transition to lower-frequency, higher-amplitude, quasi-periodic (~100-kyr) glacial variability, starting from the middle Pleistocene onwards. The five identified ILA typologies are the consequence of these shorter-lasting interglacial periods (<20 ka) compared to the longer-lasting glacial periods (100 ka). This sea level change in regime impacted and shaped coeval island shelves (Fig. 10A, C). It is well known that the width of a marine terrace is primarily dependent on the length of time that marine erosion had to carve the insular edifice (Quartau et al. 2010, 2014; Ricchi et al. 2018). Thus, the dimensions and shape of these erosional platforms are largely related to the duration of sea-level stands (Fig. 10B, D). Our ILA analysis shows that, over the last 1 Ma (cf. Fig.10A, B), marine erosion was especially prevalent in the following depth ranges: 50–60 m, where sea level stood for 13.93% of the last 1 Ma (~139.3 ka); and 70–90 m depth where it stood for 24.88% of the time (~248.8 ka). Minor differences were detected when this analysis was restricted to the last 500 ka, with the depth-bin interval of 30 to 40 m being the third most relevant (Fig. 10D). For isostatically stable islands, that is, islands that did not experience uplift or subsidence over the last 1 Ma, it is expected that the littoral area will increase whenever the 50–60 m and the 70–90 m depth ranges are crossed by the coeval [0–50] m depth limits, which serve as interval markers for calculating the ILA. This is because sea level remained at these marks for longer periods, increasing the likelihood of larger marine terraces forming within this range. Finally, it is worth emphasising that sea level was above the present datum during the most extreme interglacials (MIS 11 and MIS 5e) for only 2.49% of the last 1 Ma (~24.9 ka). Similarly, it was below 120 m depth for the same duration (2.49%, i.e., ~24.9 ka).

Hence, in theory, the sizes of ILA are dependent on the presence or absence of: 1) submarine terraces, which are first-order topographic features imprinted on the island shelf that can enlarge areas of specific depth ranges; 2) subaerial marine terraces carved high on the shores above the present sea level, during previous interglacials, or resulting from an uplift of the island; and 3) coral reefs fringing the island that, with time and accompanying the gradual sinking of the island, will transform into barrier reefs, then into an atoll, and finally, if and when corals are not able to cope with subsidence, a guyot/submerged reef bank (Menard 1984; Ramalho et al. 2013; Montaggioni and Martin-Garin 2020). However, numerous other geological factors control the insular littoral area-depth distribution on a shelf, which, in turn, influence the diverse shapes of the ILA curves.

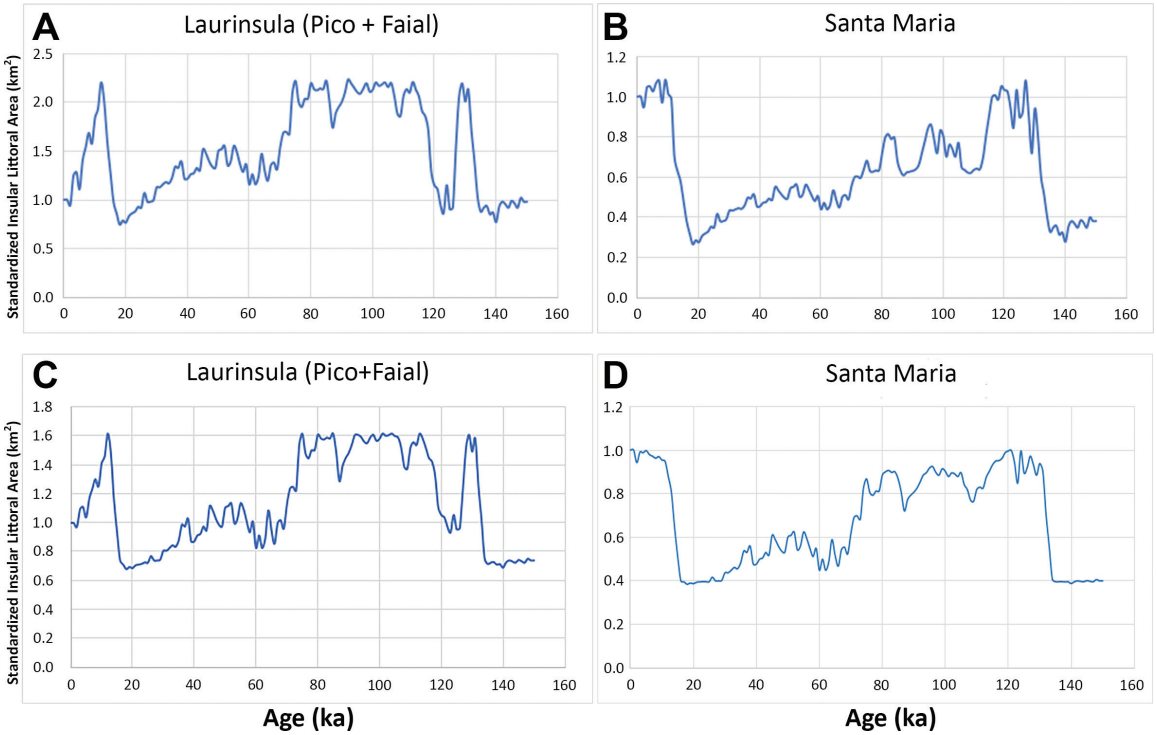

Figure 9. A, B. ILA curves using the low resolution GEBCO 2023 for (**A**) Pico+Faial (Laurinsula), an example of Soror islands (Azores Archipelago), and for (**B**) Santa Maria island in the Azores Archipelago, an example of a Solum island. **C, D**. ILA curves for Laurinsula (**C**) using a compilation of high-resolution (50 m) multibeam bathymetry (data from Quartau et al. 2015), and for Santa Maria (**D**) using a high-resolution (8 m) bathymetry (data from Ricchi et al. 2020). Note how the two pairs of curves (A/C, B/D) are similar in its general shape, suggesting that the use of the lower resolution GEBCO 2023 bathymetric dataset is sufficient to derive the relationships presented in this study.

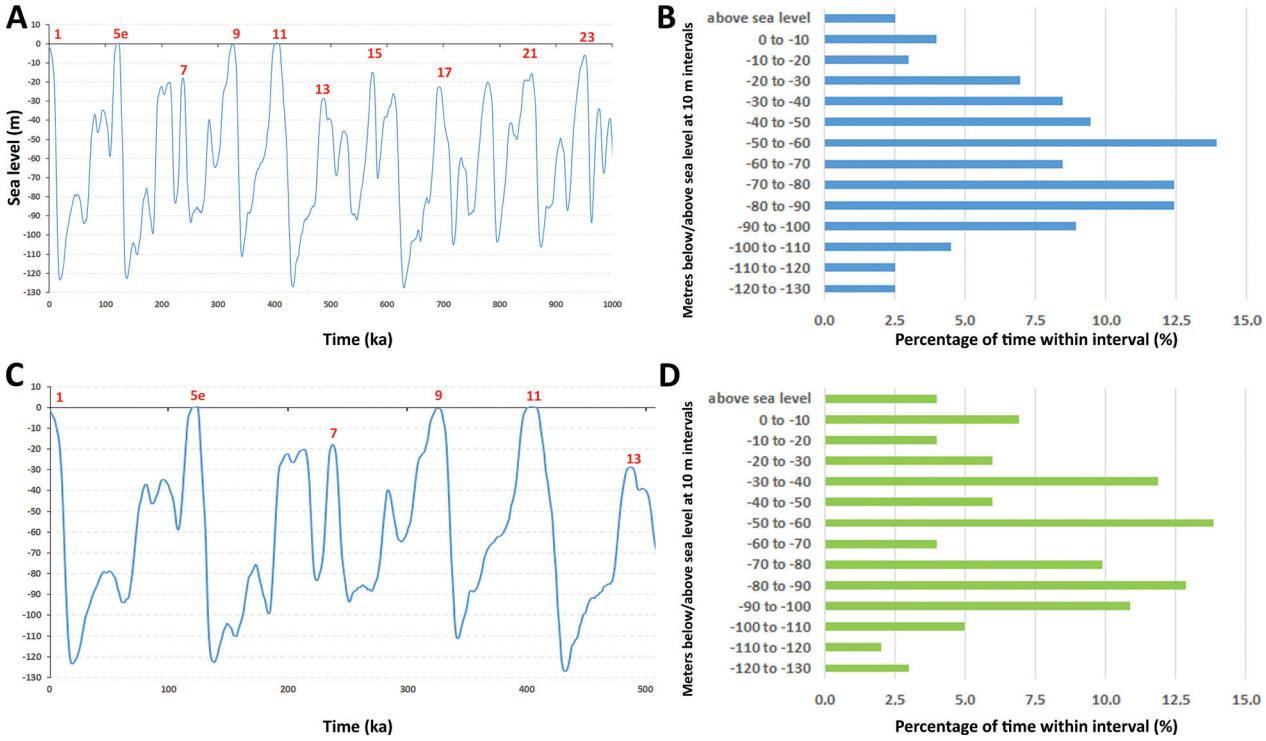

Figure 10. Characterisation of sea-level changes over the last 1 Ma (millions of years) (**A**, **B**) and over the last 500 ka (**C**, **D**). The periods of 1 Ma and 500 ka were chosen because they span ten and six full glacial-interglacial cycles, respectively. **A, C.** Sea level curve based on data from Miller et al. (2011). Numbers in red represent interglacials; ka: thousands of years. **B, D.** Quantification of the percentage of time over the last 1 Ma and 500 ka, respectively, that the sea level was within a 10-m bin interval.

For oceanic islands outside the tropics, one of the most important geological factors is island age, as the longer an island is exposed to wave erosion, the larger its shelf tends to be (Quartau et al. 2010, 2014). As depicted in Fig. 2, there is a strong correlation between island age and shelf width. However, there are other significant geological processes that also control depth distribution across the shelf, such as volcanic activity, the tectonic setting of the insular edifice (whether it is subsiding, uplifting, or isostatically stable), and the depth of the insular shelf break (Ramalho et al. 2013; Quartau et al. 2015). For subsiding islands, we can add the Darwin line effect, which occurs when tropical islands reach depths at which the temperature threshold of 20 °C required for littoral corals to continue growing is crossed. All these factors are key to explain certain patterns in littoral area curves. Additionally, these geological factors may reinforce or cancel each other's effects, making it difficult to provide general explanations.

In the case of coral reef islands, steep slopes are typically found offshore the fringing reefs or barrier reefs (Fletcher et al. 2008). Thus, a substantial increase in littoral area is expected to occur when rising sea level lead to the flooding of the large area above the edge of these reefs. Therefore, such coral reef islands conform to ILA curve type I-1 and are exemplified by the Solum island Utupua, in the Santa Cruz Islands.

Speciation on islands: a terrestrial point of view

For Solum islands, the General Dynamic Model of island biogeography (Whittaker et al. 2008, 2010) and its variants such as the Glacial Sensitive Model proposed by Fernández-Palacios et al. (2016) predict that land area, in conjunction with geological time, are the main drivers of terrestrial insular diversity. Therefore, for islands located within a tropical to temperate latitudinal range (50°S-50°N), the frequency of population splitting in the terrestrial realm will be higher during glacial periods (when the terrestrial area is maximal), whereas population merging and extinction frequencies will be higher during interglacial periods (when the land area is minimal) (Fig. 11B, Table 2). In contrast, Ali and Hutchinson (2014) showed that in the case of Soror islands of the Galápagos, the cycles of fusion-fission will be the main drivers of island diversity. Thus, in this case, a "species pump" mechanism (sensu Heaney 1985) will lead to a higher frequency of population merging during glacial periods as area and gene flow are maximal when Soror islands fuse. Moreover, the resulting larger population sizes will also increase dispersion rates among islands, contributing to an increasing frequency of population merging. Conversely, the frequency of population extinction and splitting will be higher during interglacial periods when Soror islands separate once again and their area becomes minimal (Fig. 11D, Table 2). For Moliones islands, Papadopoulou and Knowles (2017) showed that, due to the very shallow waters that separate them, the periods of island connectivity have been much longer than periods of isolation during the Quaternary. Thus, the duration of connectivity is the primary factor influencing the time available for speciation (which is not fully accomplished on these islands), overcoming the effect of area. A "species-vacuum" mechanism sensu Papadopoulou and Knowles (2017) is therefore proposed to explain the ephemeral, incipient genomic divergence of species during interglacials. Hence, although the frequency of splitting is higher during interglacials, speciation duration is longer than the period of island isolation. In Moliones islands, the frequency of population extinction and merging will therefore be higher during glacial periods (Fig. 8F, Table 2).

Extending the Sea-Level Sensitive dynamic model of marine island biogeography to include the special case of fusion-fission islands

The shift from a terrestrial point of view to a marine perspective requires a complete reversal of thought, as previously argued (e.g., Ávila et al. 2018; Freitas et al. 2019; Hachich et al. 2020; De Groeve et al. 2022). As demonstrated by Ávila et al. (2019) through their SLS dynamic model of marine island biogeography, the insular littoral area is the main driver of shallow-water marine biodiversity. Here, we expand the SLS model to include Solum, Soror, and Moliones islands and, in the process, explicitly acknowledge that connectivity in Moliones islands is fundamentally different in relation to Solum and Soror islands, as the marine connectivity within Moliones island populations of benthic, shallow water organisms is much less dependent on sea level variations when compared with Solum and Soror islands. From a marine point of view, Moliones islands behave as a single unit, and this statement is supported by the geographic distribution of *Conus* gastropods from Cabo Verde. In Cabo Verde, all the islands are Solum, except for a single group of Moliones islands composed of two islands (São Vicente and Santa Luzia) and two islets (Branco and Raso; cf. Suppl. material 1: table S3). Ávila et al. (2019) provided information on the diversity of the Cabo Verdean *Conus* species (their Suppl. material 1: table S2), reporting a total of 85 species from the archipelago, of which 70 were considered as SIME (single island marine endemics). This list was the subject of recent taxonomic re-evaluations made by the WoRMS editors, and many species were synonymized. Thus, 52 is the current number of valid *Conus* species accepted for Cabo Verde, 48 of which are endemic to the archipelago (cf. Table 3). All 48 Cabo Verdean endemic species have a non-planktotrophic mode of larval development, and 38 are considered as SIME, each of these species with a geographic distribution restricted to a single island, sometimes even confined to a bay within an island. In contrast, there are two species (*Conus pseudonivifer* Monteiro, Tenorio & Poppe,

Table 2. Frequency of population splitting, extinction, and merging in islands according to their classification (Solum, Soror, or Moliones islands) during the Last Glacial Maximum (LGM) and Last Interglacial Period (LIG)/Present time, in terrestrial and marine realms. High frequency (+), low frequency (-).

Type of Island	Glacial / Interglacial	Marine Realm			Terrestrial Realm		
		Splitting population rates (Area effect)	Extinction population rates	Merging population rates (Connectivity / Gene flow effect)	Splitting population rates (Area effect)	Extinction population rates	Merging population rates (Connectivity / Gene flow effect)
Solum	LGM	-	+++	+++	+	-	-
	LIG / Present	+++	-	-	-	+	+
Soror	LGM	-	++	++	-	-	++
	LIG / Present	++	-	-	++	++	-
Moliones	LGM	-	+	+	-	++	++
	LIG / Present	+	-	-	++	-	-

2004 and *Conus venulatus* Hwass in Bruguière, 1792) that, although being endemic to the archipelago, occur on four of the islands (Sal, Boavista, Maio, and Santiago). The interesting point here is the anomalously high number of six species (*Conus bellulus* Rolán, 1990; *Conus decoratus* Röckel, Rolán & Monteiro, 1980; *Conus grahami* Röckel, Cosel & Burnay, 1980; *Conus lugubris* Reeve, 1849; *Conus navarroi* Rolán, 1986; and *Conus saragasae* Rolán, 1986) that occur in the single Moliones group of islands, taking into account the notorious tendency for almost no dispersal of these endemic *Conus* species. In total, 11 species of *Conus* endemic to Cabo Verde are reported from this Moliones group of islands (cf. Table 3): the above-mentioned six species that occur simultaneously in São Vicente and in Santa Luzia; three other SIME *Conus* from Santa Luzia Island, and two further SIME *Conus* from São Vicente Island. Notably, there is also a group of five *Conus* species (cf. Table 3) that are shared between Boavista and Maio (both islands classified as Solum), the reason for this being the existence of a very large and shallow seamount (João Valente Bank), which highly increases the connectivity between these two Solum islands.

For Solum and Soror islands, the marine population connectivity will be lower during interglacial episodes, while isolation plays a key role in preventing gene flow among terrestrial insular populations (Papadopoulou and Knowles 2017). However, isolation is less prevalent in the marine realm (Ávila et al. 2018, 2019), primarily due to the different means of subaqueous dispersal by marine biota (larvae and eggs, as well as rafting on floating substrata by eggs/juveniles/adult organisms), and the greater connectivity of the aqueous medium in which marine organisms reside. Following the SLS dynamic model, variation in littoral area is the most prominent variable explaining the rates of marine population splitting, extinction, and merging (Ávila et al. 2019). Accordingly, across all types of islands (i.e., Solum, Soror, and Moliones), higher merging rates (due to higher gene flow) and population extinction rates (due to a minimum littoral area) are expected during glacial periods. Conversely, a higher frequency of population splitting events is expected during interglacial periods (when littoral area reaches its maximum) (Fig. 11A, C, E, Table 2). According to our data, these expectations occur in 82 of the 102 analysed islands or groups of islands; cf. Table 1). Thus, the assumptions of the SLS dynamic model are sustained in 80.4% of the 102 analysed cases, with synergetic effects of small littoral area and high gene flow wiping out or merging incipient lineages more frequently during glacial periods. However, the gradient of variation in the islands' littoral area during glacial and interglacial periods, as identified here by the ILA curves, has a bearing on the frequency of speciation processes (i.e., population splitting, extinction, and merging): Solum islands have comparatively higher differences in littoral area and frequency of processes driving speciation events (Fig. 11A), followed by Soror islands with intermediate levels (Fig. 11C), and, finally, by Moliones islands with lower levels of speciation processes taking place (Fig. 11E). Again, the endemic Cabo Verdean *Conus* support our predictions, with a higher number of species registered in the Solum islands (17 endemic *Conus* at Boavista Island, 15 at Maio, and 10 at Sal) when compared with the Moliones islands (9 endemic *Conus* at Santa Luzia and 8 at São Vicente; cf. Table 3).

Although Ávila et al. (2018) found that the changes in isolation caused by glacial-interglacial cycles are negligible for most Atlantic archipelagos, the amount of time available for speciation (i.e., the period of ILA isolation) is crucial for differentiating Solum, Soror, and Moliones islands. As previously stated, the ILA has an increasing effect on the connectivity between islands, being minimal in Solum islands, intermediate in Soror islands, and reaching a maximal effect in Moliones islands. In the case of Moliones islands, no significant changes in the high values of connectivity within these islands are expected in the marine realm, with biodiversity being essentially independent of glacial-interglacial cycles (cf. Figs 3–5). The importance of island connectivity is thus ranked as medium to low in the case of Solum islands, and very relevant in the case of Soror islands.

Table 3. Geographic distribution per island and total number of *Conus* species per island in the Cabo Verde archipelago. Data reviewed from the Suppl. material 1: table S2 of Ávila et al. (2019).

Species of *Conus* endemic to Cabo Verde	Santo Antão	São Vicente	Santa Luzia	São Nicolau	Sal	Boavista	Maio	Santiago	Fogo	Brava
Conus antoniaensis (T. Cossignani & Fiadeiro, 2014)						1				
Conus antoniomonteiroi Rolán, 1990					1					
Conus ateralbus Kiener, 1850					1					
Conus bellulus Rolán, 1990		1	1							
Conus boavistensis Rolán & F. Fernandes, 1990						1				
Conus borgesi Trovão, 1979						1				
Conus calhetae Rolán, 1990							1			
Conus crotchii Reeve, 1849						1				
Conus cuneolus Reeve, 1843					1					
Conus curralensis Rolán, 1986			1							
Conus damottai Trovão, 1979						1	1			
Conus decoratus Röckel, Rolán & Monteiro, 1980		1	1							
Conus delanoyae Trovão, 1979						1				
Conus denizi (Afonso & Tenorio, 2011)		1								
Conus diminutus Trovão & Rolán, 1986						1				
Conus espingueirensis (T. Cossignani & Fiadeiro, 2017)						1				
Conus felitae Rolán, 1990					1					
Conus fernandesi Tenorio, Afonso & Rolán, 2008	1									
Conus freitasi (Tenorio, Afonso, Rolán, Pires, Vasconcelos, Abalde & Zardoya, 2018)		1								
Conus furnae Rolán, 1990										1
Conus fuscoflavus Röckel, Rolán & Monteiro, 1980						1	1			
Conus galeao Rolán, 1990							1			
Conus gonsaloi (Afonso & Tenorio, 2014)							1			
Conus grahami Röckel, Cosel & Burnay, 1980		1	1							
Conus infinitus Rolán, 1990							1			
Conus insulae (Tenorio, Abalde, Pardos-Blas & Zardoya, 2020)			1							
Conus isabelarum Tenorio & Afonso, 2004							1			
Conus josephinae Rolán, 1980						1	1			
Conus kersteni Tenorio, Afonso & Rolán, 2008				1						
Conus longilineus Röckel, Rolán & Monteiro, 1980					1					
Conus lugubris Reeve, 1849		1	1							
Conus maioensis Trovão, Rolán & Félix-Alves, 1990						1	1			
Conus marimaris (Tenorio, Abalde & Zardoya, 2018)					1					
Conus miruchae Röckel, Rolán & Monteiro, 1980					1					
Conus navarroi Rolán, 1986		1	1							
Conus perrineae (T. Cossignani & Fiadeiro, 2018)							1			
Conus pseudonivifer Monteiro, Tenorio & Poppe, 2004					1	1	1	1		
Conus raulsilvai Rolán, Monteiro & C. Fernandes, 1998							1			
Conus regonae Rolán & Trovão, 1990					1					
Conus roeckeli Rolán, 1980						1				
Conus salletae (T. Cossignani, 2014)						1				
Conus santaluziensis (T. Cossignani & Fiadeiro, 2015)			1							
Conus santanaensis (Afonso & Tenorio, 2014)							1			
Conus saragasae Rolán, 1986		1	1							
Conus trochulus Reeve, 1844						1	1			
Conus venulatus Hwass in Bruguière, 1792					1	1	1	1		
Conus verdensis Trovão, 1979								1		
Conus vulcanus Tenorio & Afonso, 2004						1				
Number of endemic species of *Conus*/island	**1**	**8**	**9**	**1**	**10**	**17**	**15**	**3**	**0**	**1**
***Species of Conus* not endemic to Cabo Verde**										
Conus ambiguus Reeve, 1844		1			1	1				
Conus ermineus Born, 1778	1	1	1	1	1	1	1	1		
Conus genuanus Linnaeus, 1758		1					1			
Conus tabidus Reeve, 1844	1				1	1	1			
Total number of *Conus* species/island	**3**	**11**	**10**	**2**	**13**	**20**	**18**	**4**	**0**	**1**

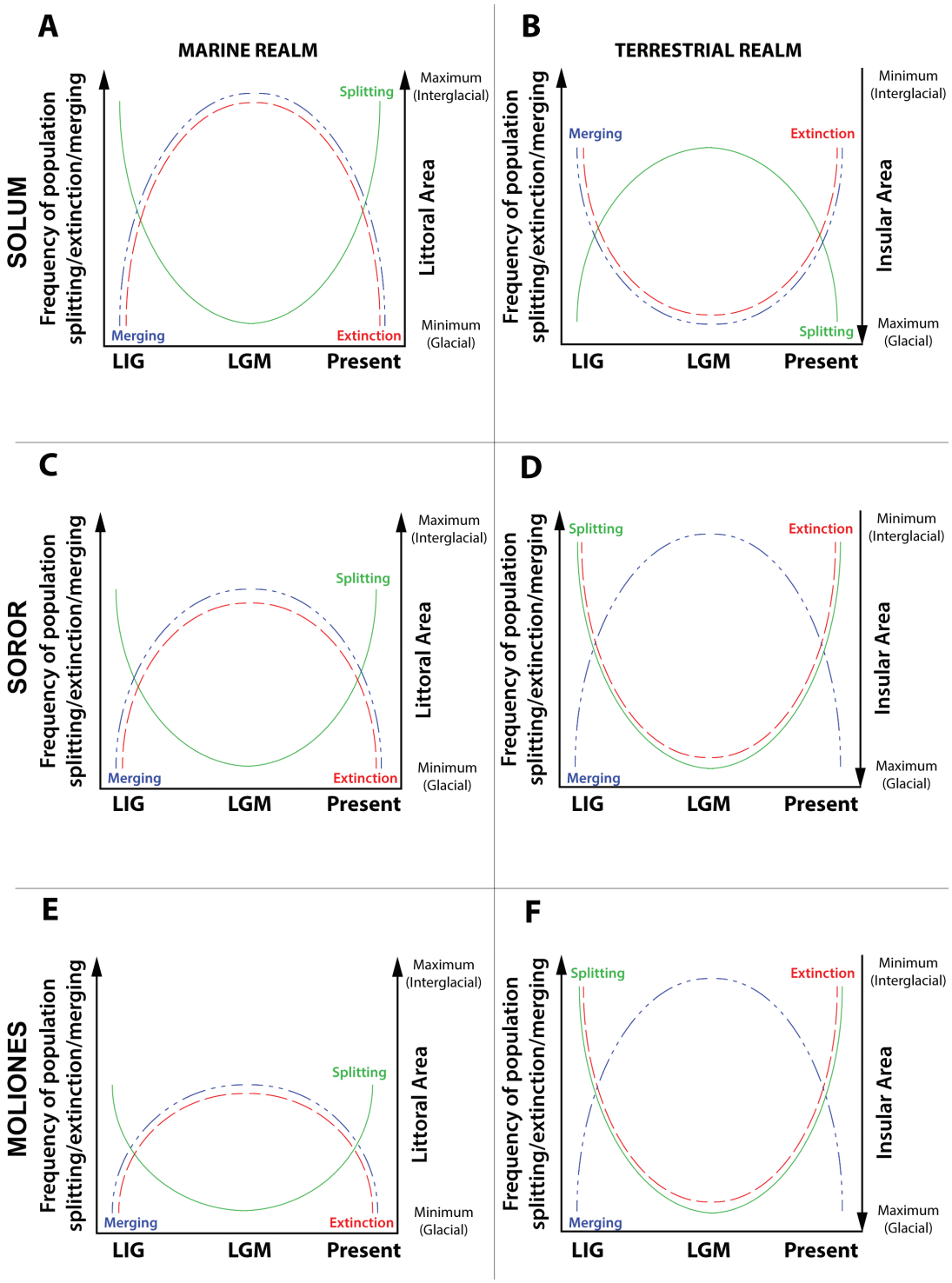

Figure 11. Comparison between marine and terrestrial realms, regarding the predicted effects of glacial-interglacial cycles and the associated sea-level fluctuations on the three main processes that regulate the frequency of speciation on Solum islands (A-B), Soror islands (C-D), and Moliones islands (E-F). Please note that in the case of the marine realm, there are quantitative differences in the frequency levels of population splitting (shown in green), population extinction (red), and population merging (blue), with higher values in Solum islands, intermediate values in Soror islands, and lower values in Moliones islands. Also, in the marine realm, the frequency of population extinction and merging attain their maximum values during glacial periods for all types of islands, which contrasts with the pattern for the terrestrial realm (see Papadopoulos and Knowles 2015). The predictions for the terrestrial realm fall under two models: in B, it is depicted the relative values of the frequencies when shifts in island area are considered as the main driver of island diversity patterns (MacArthur and Wilson 1967; Fernández-Palacios et al. 2016), and where the frequency of population splitting reaches its maximum during glacial episodes; in D and F, it is expressed the relative variation of the frequencies of population splitting, extinction, and merging, when the cycles of fusion-fission are considered as the main driver of island diversity through a "species pump" mechanism (Heaney 1985; Ali and Aitchison 2014); in this case, it is the frequency of population merging that reaches its maximum during glacial episodes.

Nevertheless, as the sea level falls during the inception of a glacial episode, the littoral area of Moliones islands suddenly decreases when the sea level falls below the shallow depths that separate these islands. When this occurs, the initial terrestrial area of the island, along with the coastal region, becomes entirely subaerial, resulting in a sudden decrease in insular littoral area. Moreover, the littoral area of Moliones islands tends to persist at low levels for extended periods compared to Soror or Solum islands. This helps explain why the frequencies of population splitting, extinction, and merging are comparatively higher in Solum islands (Fig. 11A), intermediate in Soror islands (Fig. 11C), and lower in Moliones islands (Fig. 11E).

Genetic population divergence versus species diversification

In marine ILA habitats, the process of speciation hinges significantly on the duration of isolation (see Fig. 1). Over evolutionary timescales, while complete speciation might not occur universally, genetic divergence among populations is expected, with its extent likely influenced by the type of island. Papadopoulou and Knowles (2015) demonstrated that the high levels of genomic divergence detected in Caribbean crickets across the Virgin Islands, which are associated with repeated connectivity cycles, do not translate into species diversification. Taking all of the above into consideration, we predict a genetic population divergence-pump effect for the ILA habitats, with higher genetic population diversity in Moliones islands, and progressively, comparatively smaller genetic diversity values in Soror islands, and even smaller in Solum islands. In contrast, we predict the frequency of population-exclusive haplotypes to be higher in Solum islands than in those experiencing fusion-fission cycles (i.e., Soror- and Moliones islands). This expectation arises from the assumption that dispersal and gene flow are expected to be lower in Solum islands due to prolonged isolation. This extended period of isolation provides ample time for new genetic variants to emerge within the population and gradually increase in frequency over time, ultimately becoming exclusive to that population. At the other extreme, Moliones islands are always connected through time, continuously exchanging individuals and likely working either as a single population or as a marine metapopulation (Kritzer and Sale 2006) during interglacial periods. This connectivity reduces the likelihood of the appearance of new exclusive haplotypes. Soror islands constitute an intermediate case, where connectivity and gene flow levels follow a pulse-like trend during glacial-interglacial cycles, alternating between continuous and fragmented habitats. During interglacial periods, these are separated by unsuitable, deep-water habitats which hamper connectivity among populations, causing a certain degree of isolation and allowing for the occasional appearance of new haplotypes within each island or population. The fusion of islands during glacial periods ensures the physical continuity of shallow-water habitats and allows individuals to be exchanged, thus increasing overall genetic diversity. When the next interglacial period starts, the habitat undergoes fragmentation once more, resulting in the interruption or, at the very least, reduction of gene flow.

Bernardi et al. (2014) studied the phylogeography of the Galápagos' reef fishes, whereas Almada et al. (2017) studied the phylogeography of the ballan wrasse *Labrus bergylta* Ascanius, 1767 across its distribution range, and Baptista et al. (2021) studied the population structure of the intertidal gastropod *Cingula trifasciata* (J. Adams, 1800) in the Azores Archipelago. Their results support our predictions. The six insular reef fish species studied by Bernardi et al. (2014) [*Lythrypnus gilberti* (Heller & Snodgrass, 1903), *Dialommus fuscus* Gilbert, 1891, *Lepidonectes corallicola* (Kendall & Radcliffe, 1912), *Malacoctenus zonogaster* Heller & Snodgrass, 1903, *Stegastes beebei* (Nichols, 1924), and *Stegastes arcifrons* (Heller & Snodgrass, 1903)] consistently show higher frequency of exclusive haplotypes in Solum islands (e.g., San Cristobal, Española, Marchena, and Wolf), when compared with the Soror islands (Fernandina+Isabela; cf. fig. 2 of Bernardi et al. 2014). In the Azores, the populations of *Labrus bergylta* studied by Almada et al. (2017) also show higher frequency of exclusive haplotypes in Solum islands (e.g., Santa Maria, Corvo), when compared with the group of Soror islands (Faial+Pico (although Pico was not sampled); cf. figs 2, 3 of Almada et al. 2017). In a similar manner, the populations of the intertidal gastropod studied by Baptista et al. (2021) also show higher frequency of exclusive haplotypes in four out of the five Solum islands sampled, when compared with the group of Soror islands (Pico+Faial (although Faial was not sampled); cf. fig. 3 of Baptista et al. 2021).

Conclusions

This study extends the SLS dynamic model of marine island biogeography and, for the first time, elucidates the evolutionary dynamics affecting shallow-water marine biota as a consequence of island fusion-fission cycles driven by sea-level changes. Building on Ávila et al. (2019) ontogenetic classification of volcanic oceanic islands that delineates a progression from young to old islands, this study introduces a classification system applicable to other types of oceanic islands (e.g., coral islands) and to continental shelf islands, categorising islands and island groups as Solum, Soror, or Moliones. This new classification incorporates the variation of the depth distribution across the shelf, which significantly influences marine evolutionary processes and associated biogeographic patterns.

Variations in the insular littoral area (ILA) in response to sea-level fluctuations during glacial-interglacial cycles are expressed in five general types of ILA curves, depending on the diverse shelf area-depth distribution. Among these, three curves (I-1, I-2 and I-3) peaked in littoral area

during interglacial periods, while the remaining two curves (G-1 and G-2) reached maximum values during glacial periods. The majority of the islands and groups of islands examined in this study conformed to the predictions of the SLS dynamic model, with 78% of Solum islands, 80% of Soror islands, and 84% of Moliones islands aligned with the model. For these three categories of islands, we explain why a higher frequency of splitting population events is expected during interglacial periods, whereas higher population merging and extinction rates are expected during glacial periods. Similarly, we show that the projected impacts of littoral area changes on islands during glacial and interglacial periods are contingent upon the island type. Solum islands exhibit relatively greater disparities in littoral area and frequency of processes driving speciation events, followed by Soror islands with intermediate levels, and finally, Moliones islands. In addition, we suggest that the frequencies of population splitting, extinction, and merging are comparatively higher in Solum islands, intermediate in Soror islands, and lower in Moliones islands. Finally, under similar population sizes, a higher connectivity (gene flow) should be expected on Moliones and Soror islands, thus favouring genetic diversity while spreading endemic lineages, decreasing the rates of single island marine endemics.

In conclusion, we suggest that genetic divergence among shallow-water marine populations is influenced by the type of island (Solum, Soror, or Moliones), and we predict a genetic population divergence-pump effect, expecting greater genetic population diversity in Moliones islands, followed by comparatively lower diversity in Soror islands, and even less in Solum islands. We also predict a higher frequency of population-exclusive haplotypes in Solum islands compared to islands subjected to fusion-fission cycles (i.e., Soror and Moliones islands).

Acknowledgements

We acknowledge the helpful comments made by two reviewers (Hudson Pinheiro and José María Fernández-Palacios), who contributed to clarify relevant sections of this manuscript. SPA and PM acknowledge their contracts with project M1.1. A/ INFRAEST CIENT/A/001/2021 - Base de Dados da PaleoBiodiversidade da Macaronésia, funded by the Regional Government of the Azores. SPA appreciates his current FCT/2023.07418 CEEECIND research contract with BIOPOLIS. CSM and LB benefited from PhD grants funded by the Regional Government of the Azores (M3.1.a/F/100/2015) and the Portuguese FCT (Fundação para a Ciência e Tecnologia) Agency (SRFH/BD/135918/2018), respectively. AP holds a CEEC Institutional grant https://doi.org/10.54499/CEECINST/00024/2021/CP2780/CT0003, funded by FCT. This work also benefited from FEDER funds, through the Operational Program for Competitiveness Factors – COMPETE, and from National Funds, through FCT (UIDB/50027/2020, POCI-01–0145-FEDER-006821, UIDB/00153/2020, LA/P/0048/2020), as well as through the Regional Government of the Azores (M1.1.a/005/Funcionamento-C-/2016, CIBIO-A; M1.1.A/INFRAEST CIENT/A/001/2021; M3.3.B/ORG.R.C./005/2021, M3.3.B/ORG.R.C./008/2022/EDIÇÃO 1, M3.3.G/EXPEDIÇÕES CIENTÍFICAS/005/2022 and M3.3.G/EXPEDIÇÕES CIENTÍFICAS/004/2022). Finally, this work was also supported by FEDER funds (85%) and by funds from the Regional Government of the Azores (15%) through the Azores 2020 Operational Program under the VRPROTO project: Virtual Reality PROTOtype: the geological history of "Pedra- que-pica": ACORES-01-0145-FEDER-000078, and by M1.1.A/INFRAEST CIENT/A/001/2021 - Base de Dados da PaleoBiodiversidade da Macaronésia.

Credit Authorship Contribution Statement

SPA: Conceptualization, Funding acquisition, Investigation, Data curation, Methodology, Formal Analysis, Resources, Supervision, Validation, Visualization, Writing - original draft, Writing – review and editing. CSM: Investigation, Data curation, Visualization, Writing – review and editing. JMP, AMM: Methodology, Formal Analysis, Writing – review and editing. RQ, RSR: Formal Analysis, Validation, Writing – review and editing. AMS, LB, AP, PM, ACR, AH, SEV, GCA, MM, BB, KFR, EM-G, MEJ: Writing – review and editing.

Declaration of Interests

The authors declare that they have no known competing financial interests or personal relationships that could have appeared to influence the work reported in this paper.

References

Ali JR, Aitchison JC (2014) Exploring the combined role of eustasy and oceanic island thermal subsidence in shaping biodiversity on the Galápagos. Journal of Biogeography 41: 1227–1241. https://doi.org/10.1111/jbi.12313

Almada F, Francisco SM, Lima, CS, FitzGerald R, Mirimin L, Villegas-Ríos D, Saborido-Rey F, Afonso P, Morato T, Bexiga S, Robalo JI (2017) Historical gene flow constraints in a northeastern Atlantic fish: phylogeography of the ballan wrasse *Labrus bergylta* across its distribution range. Royal Society Open Science 4: 160773. https://doi.org/10.1098/rsos.160773

Ávila SP (2006) Oceanic islands, rafting, geographical range and bathymetry: a neglected relationship? Occasional Publication of the Irish Biogeographical Society 9: 22–39.

Ávila SP (2013) Unravelling the patterns and processes of evolution of marine life in oceanic islands: a global framework. In: Fernández-Palacios JM, Nascimento L, Hernández JC, Clemente S, González A, Díaz-González JP (Eds) Climate Change perspectives from the Atlantic: past, present and future. Universidad de La Laguna, Tenerife, 95–125.

Ávila SP, Cordeiro R, Haroun R, Wirtz P (2016) Comment on "Island biogeography: patterns of marine shallow-water organisms" by Hachich et al. Journal of Biogeography (2015). Journal of Biogeography 43: 2515–2516. https://doi.org/10.1111/jbi.12816

Ávila SP, Cordeiro R, Madeira P, Silva L, Medeiros A, Rebelo AC, Melo C, Neto AI, Haroun R, Monteiro A, Rijsdijk K, Johnson ME (2018) Global change impacts on large-scale biogeographic patterns of marine organisms on Atlantic oceanic islands. Marine Pollution Bulletin 126: 101–112. https://doi.org/10.1016/j.marpolbul.2017.10.087

Ávila SP, Melo C, Sá N, Quartau R, Rijsdijk K, Ramalho RS, Berning B, Cordeiro R, de Sá NC, Pimentel A, Baptista L, Medeiros A, Gil A, Johnson ME (2019) Towards a "Sea-Level Sensitive Marine Island Biogeography" model: the impact of glacio-eustatic oscillations in global marine island biogeographic patterns. Biological Reviews 94 (3): 1116–1142. https://doi.org/10.1111/brv.12492

Baptista L, Santos AM, Cabezas MP, Cordeiro R, Melo C, Ávila SP (2019) Intertidal or subtidal/circalittoral species: who appeared first? A phylogenetic approach to the evolution of non-planktotrophic species in Atlantic Archipelagos. Marine Biology 166: 88. https://doi.org/10.1007/s00227-019-3536-y

Baptista L, Meimberg H, Ávila SP, Santos AM, Curto M (2021) Dispersal ability, habitat characteristics, and sea-surface circulation shape population structure of *Cingula trifasciata* (Gastropoda: Rissoidae) in the remote Azores Archipelago. BMC Ecology and Evolution 21: 128. https://doi.org/10.1186/s12862-021-01862-1

Bernardi G, Ramon, ML, Alva-Campbell Y, McCosker JE, Bucciarelli G, Garske LE, Victor BC, Crane NL (2014) Darwin's fishes: phylogeography of Galápagos Islands reef fishes. Bulletin of Marine Science 90(1): 533–549. https://doi.org/10.5343/bms.2013.1036

Dynesius M, Jansson R (2000) Evolutionary consequences of changes in species' geographical distributions driven by Milankovitch climate oscillations. Proceedings of the National Academy of Sciences, USA 97: 9115–9120. https://doi.org/10.1073/pnas.97.16.9115

Fernández-Palacios JM, Ridjsdiijk KF, Norder SJ, Otto R, de Nascimento L, Fernández-Lugo S, Tjørve E, Whittaker RJ (2016) Towards a glacial-sensitive model of Island biogeography. Global Ecology and Biogeography 25: 817–830. https://doi.org/10.1111/geb.12320

Fletcher CH, Bochicchio C, Conger CL, Engels MS, Feirstein EJ, Frazer N, Glenn CR, Grigg RW, Grossman EE, Harney JN, Isoun E, Murray-Wallace CV, Rooney JJ, Rubin KH, Sherman CE, Vitousek S (2008) Geology of Hawaii reefs. Chapter 11. In: Riegl BM, Dodge RE (Eds) Coral reefs of the USA. Coral reefs of the world 1. Springer, New York, 435–488. https://doi.org/10.1007/978-1-4020-6847-8_11

Florencio M, Patiño J, Nogué S, Traveset A, Borges PAV, Schaefer H, Amorim IR, Arnedo M, Ávila SP, Cardoso P, Nascimento L de, Fernández-Palacios JM, Gabriel SI, Gil A, Gonçalves V, Haroun R, Illera JC, López-Darias M, Martínez A, Martins GM, Neto AI, Nogales M, Oromí P, Rando JC, Raposeiro PM, Rigal F, Romeiras M, Silva L, Valido A, Vanderpoorten A, Vasconcelos R, Santos AMC (2021) Macaronesia as a fruitful arena for Ecology, Evolution and Conservation Biology. Frontiers in Ecology and Evolution 9: 718169. https://doi.org/10.3389/fevo.2021.718169

Freitas R, Romeiras M, Silva L, Cordeiro R, Madeira P, González JA, Wirtz P, Falcón JM, Brito A, Floeter SR, Afonso P, Porteiro F, Vieira-Rodríguez MA, Neto AI, Haroun R, Farminhão JNM, Rebelo AC, Baptista L, Melo CS, Martínez A, Nuñez J, Berning B, Johnson ME, Ávila SP (2019) Restructuring of the "Macaronesia" biogeographic unit: a marine multi-taxon biogeographical approach. Scientific Reports 9: 15792. https://doi.org/10.1038/s41598-019-51786-6

GDAL/OGR contributors (2023) GDAL/OGR Geospatial Data Abstraction software Library. Open Source Geospatial Foundation. https://gdal.org

GEBCO (2023) GEBCO. https://www.gebco.net/data_and_products/gridded_bathymetry_data

Groeve J de, Kusumoto B, Koene E, Kissling WD, Seijmonsbergen AC, Hoeksema BW, Yasuhara M, Norder SJ, Cahyarini SY, van der Geer A, Meijer HJM, Kubota Y, Rijsdijk KF (2022) Global raster dataset on historical coastline positions and shelf sea extents since the Last Glacial Maximum. Global Ecology and Biogeography 31(11): 2162–2171. https://doi.org/10.1111/geb.13573

Hachich NF, Bonsall MB, Arraut EM, Barneche DR, Lewinsohn TM, Floeter SR (2015) Island biogeography: Patterns of marine shallow-water organisms in the Atlantic Ocean. Journal of Biogeography 45: 1871–1882. https://doi.org/10.1111/jbi.12560

Hachich NF, Bonsall MB, Arraut EM, Barneche DR, Lewinsohn TM, Floeter SR (2016) Marine island biogeography. Response to comment on 'Island biogeography: Patterns of marine shallow-water organisms. Journal of Biogeography 43: 2517–2519. https://doi.org/10.1111/jbi.12863

Hachich NF, Ferrari DS, Quimbayo JP, Pinheiro HT, Floeter SR (2020) Island biogeography of marine shallow-water organisms. Encyclopedia of the World's Biomes 1: 61–75. https://doi.org/10.1016/B978-0-12-409548-9.11947-5

Hammoud C, Kougioumoutzis K, Rijsdijk KF, Simaiakis SM, Norder SJ, Foufopoulos J, Georgopoulou E, van Loon EE (2021) Past connections with the mainland structure patterns of insular species richness in a continental shelf archipelago (Aegean Sea, Greece). Ecology and Evolution 11(10): 5441–5458. https://doi.org/10.1002/ece3.7438

Heaney LR (1985) Zoogeographic evidence for middle and late Pleistocene land bridges to the Philippine Islands. Modern Quaternary Research in Southeast Asia 9: 127–144.

Kritzer JP, Sale PF (2006) Marine Metapopulations. Academic Press, Burlington, MA, USA.

Ludt WB, Rocha LA (2015) Shifting seas: the impacts of Pleistocene sea-level fluctuations on the evolution of tropical marine taxa. Journal of Biogeography 42: 25–38. https://doi.org/10.1111/jbi.12416

MacArthur RH, Wilson EO (1963) An equilibrium theory of insular zoogeography. Evolution 17: 373–387. https://doi.org/10.2307/2407089

MacArthur RH, Wilson EO (1967) The theory of island biogeography. Princeton Univ. Press, Princeton, New Jersey.

Melo CS, Martín-González E, Silva CM da, Galindo I, González-Rodríguez A, Baptista L, Rebelo AC, Madeira P, Voelker AHL, Johnson ME, Arruda SA, Ávila SP (2022) Range expansion of tropical shallow-water marine molluscs in the NE Atlantic during the last interglacial (MIS 5e): Causes, consequences and utility of ecostratigraphic indicators for the Macaronesian archipelagos. Quaternary Science Reviews 278: 107377. https://doi.org/10.1016/j.quascirev.2022.107377

Melo CS, Silva CM da, Scarponi D, Martín-González E, Rolán E, Rojas A, Martinez S, Silva L, Johnson M, Rebelo AC, Baptista L, Voelker A, Ramalho RS, Ávila SP (2023) Palaeobiogeography of NE Atlantic archipelagos during the Last Interglacial (MIS 5e): A molluscan approach to the conundrum of Macaronesia as a marine biogeographic unit. Quaternary Science Reviews 319: 108313. https://doi.org/10.1016/j.quascirev.2023.108313

Menard HW (1984) Origin of guyots: the Beagle to Seabeam. Journal of Geophysics Research 89: 11117–11123. https://doi.org/10.1029/JB089iB13p11117

Miller KG, Mountain GS, Wright JD, Browning JV (2011) A 180-Million-Year Record of Sea Level and Ice Volume Variations from Continental Margin and Deep-Sea Isotopic Records. Oceanography 24(2): 40–53. https://doi.org/10.5670/oceanog.2011.26

Montaggioni L, Martin-Garin B (2020) A brief geological story of French Polynesia. In: Boutet M, Gourguet R, Letourneux J (Eds) Marine Molluscs of French Polynesia, Au Vent des Îles Editions, Université de Polynésie française, 38–43.

Norder SJ, Proios K, Whittaker RJ, Alonso MR, Borges PAV, Borregaard MK, Cowie RH, Florens FBV, Martins AMF, Ibáñez M, Kissiling WD, de Nascimento L, Otto R, Parent CE, Rigal F, Warren BH, Fernández-Palacios JM, van Loon EE, Triantis KA, Rijsdijk KF (2019) Beyond the Last Glacial Maximum: Island endemism is best explained by long lasting archipelago configurations. Global Ecology and Biogeography 28(2): 184–197. https://doi.org/10.1111/geb.12835

Papadopoulou A, Knowles LL (2015) Genomic tests of the species-pump hypothesis: Recent island connectivity cycles drive population divergence but not speciation in Caribbean crickets across the Virgin Islands. Evolution 69(6): 1501–1517. https://doi.org/10.1111/evo.12667

Papadopoulou A, Knowles LL (2017) Linking micro- and macroevolutionary perspectives to evaluate the role of Quaternary sea-level oscillations in island diversification. Evolution 71-72: 2901–2917. https://doi.org/10.1111/evo.13384

Patiño J, Whittaker RJ, Borges PAV, Fernández-Palacios JM, Ah-Peng C, Araújo M, Ávila SP, Cardoso P, Cornuault J, de Boer EJ, de Nascimento L, Gil A, González-Castro A, Gruner DS, Heleno R, Hortal J, Illera JC, Kaiser-Bunbury C, Matthews T, Papadopoulou A, Pettorelli N, Price JP, Santos AMC, Steinbauer MJ, Triantis KA, Valente L, Vargas P, Weigelt P, Emerson BC (2017) A roadmap for island biology: 50 fundamental questions after 50 years of The Theory of Island Biogeography. Journal of Biogeography 44: 963–983. https://doi.org/10.1111/jbi.12986

Pinheiro HT, Bernardi G, Simon T, Joyeux J-C, Macieira RM, Gasparini JL, Rocha C, Rocha LA (2017) Island biogeography of marine organisms. Nature 82: 82–86. https://doi.org/10.1038/nature23680

QGIS.org (2023) QGIS Geographic Information System. Open Source Geospatial Foundation Project. http://qgis.org

Quartau R, Trenhaile AS, Mitchell NC, Tempera F (2010) Development of volcanic insular shelves: insights from observations and modelling of Faial Island in the Azores archipelago. Marine Geology 275: 66–83. https://doi.org/10.1016/j.margeo.2010.04.008

Quartau R, Hipólito A, Romagnoli C, Casalbore D, Madeira J, Tempera F, Roque C, Chiocci FL (2014) The morphology of insular shelves as a key for understanding the geological evolution of volcanic islands: insights from Terceira Island (Azores). Geochemistry, Geophysics, Geosystems 15: 1801–1826. https://doi.org/10.1002/2014GC005248

Quartau R, Madeira J, Mitchell NC, Tempera F, Silva PF, Brandão F (2015) The insular shelves of the Faial-Pico Ridge: a morphological record of its geologic evolution (Azores archipelago). Geochemistry, Geophysics, Geosystems 16: 1401–1420. https://doi.org/10.1002/2015GC005733

Quartau R, Madeira J, Mitchell NC, Tempera F, Silva PF, Brandão F (2016) Reply to comment by Marques et al. on "The insular shelves of the Faial-Pico Ridge (Azores archipelago): A morphological record of its evolution". Geochemistry, Geophysics, Geosystems 17: 633–641. https://doi.org/10.1002/2015GC006180

Quartau R, Trenhaile AS, Ramalho RS, Mitchell NC (2018) The role of subsidence in shelf widening around ocean island volcanoes: Insights from observed morphology and modeling. Earth and Planetary Science Letters 498: 408–417. https://doi.org/10.1016/j.epsl.2018.07.007

Ramalho RS, Quartau R, Trenhaile AS, Mitchell NC, Woodroffe CD, Ávila SP (2013) Coastal evolution on volcanic oceanic islands: A complex interplay between volcanism, erosion, sedimentation, sea-level change and biogenic production. Earth-Science Reviews 127: 140–170. https://doi.org/10.1016/j.earscirev.2013.10.007

Ricchi A, Quartau R, Ramalho RS, Romagnoli C, Casalbore D, da Cruz JV, Fradique C, Vinhas A (2018) Marine terrace development on reefless volcanic islands: New insights from high-resolution marine geophysical data offshore Santa Maria Island (Azores Archipelago). Marine Geology 406: 42–56. https://doi.org/10.1016/j.margeo.2018.09.002

Ricchi A, Quartau R, Ramalho RS, Romagnoli C, Casalbore D (2020) Imprints of volcanic, erosional, depositional, tectonic and mass-wasting processes in the morphology of Santa Maria insular shelf. Marine Geology 424: 106163. https://doi.org/10.1016/j.margeo.2020.106163

Rijsdijk KF, Hengl T, Norder S, Otto R, Emmerson BC, Ávila SP, López H, van Loon EE, Tjorve E, Fernández-Palacios JM (2014) Quantifying surface area changes of volcanic islands driven by Pleistocene sea level cycles: biogeographic implications for Macaronesian archipelagos, Atlantic Ocean. Journal of Biogeography 41(7): 1242–1254. https://doi.org/10.1111/jbi.12336

Sacchetti C, Landau B, Ávila SP (2023) The Lower Pliocene marine gastropods of Santa Maria Island, Azores: Taxonomy and palaeobiogeographic implications. Zootaxa 5295(1): 1–150. https://doi.org/10.11646/zootaxa.5295.1.1

Simaiakis SM, Rijsdijk KF, Koen EFM, Norder SJ, van Boxel JH, Stocchi P, Hammoud C, Kougioumoutzis K, Georgopoulou E, van Loon E, Tjørve KMC, Tjørve E (2017) Geographic changes in the Aegean Sea since the Last Glacial Maximum: Postulating biogeographic effects of sea-level rise on islands. Palaeogeography, Palaeoclimatology, Palaeoecology 471: 108–119. https://doi.org/10.1016/j.palaeo.2017.02.002

Tittley I, Álvaro NV, Neto AI (2014) Preliminary observations on the benthic marine algae of the Gorringe seabank (northeast Atlantic Ocean). Helgoland Marine Research 68: 307–312. https://doi.org/10.1007/s10152-014-0391-6

Whittaker RJ, Triantis KA, Ladle RJ (2008) A general dynamic theory of oceanic Island biogeography. Journal of Biogeography 35: 977–994. https://doi.org/10.1111/j.1365-2699.2008.01892.x

Whittaker RJ, Triantis KA, Ladle RJ (2010) A general dynamic theory of oceanic island biogeography: extending the MacArthur-Wilson theory to accommodate the rise and fall of volcanic islands. In: Losos JBM, Ricklefs RE (Eds) The Theory of Island Biogeography revisited, Princeton University Press, Princeton, 88–115. https://doi.org/10.1515/9781400831920.88

Supplementary materials

Supplementary material 1

Additional tables and figures (.docx)

Link: https://doi.org/10.21425/fob.18.141200.suppl1